International Journal of Mass Spectrometry 276 (2008) 56–76

Contents lists available at ScienceDirect

International Journal of Mass Spectrometry

journal homepage: www.elsevier.com/locate/ijms

Halogenated silanes, radicals, and cations: Theoretical predictions on ionization energies, structures and potential energy surfaces of cations, proton affinities, and enthalpies of formation

Liming Wang*, Yi-Liang He

College of Chemistry and Chemical Engineering, South China University of Technology, Guangzhou 510640, PR China

ARTICLE INFO

Article history:
Received 4 June 2008
Received in revised form 10 July 2008
Accepted 11 July 2008
Available online 22 July 2008

Keywords:
Halosilanes
Ionization energy
Proton affinity
Enthalpy of formation

ABSTRACT

Quantum chemistry study has been carried out on the structure and energetics of halogenated silanes, radicals, and cations ($SiH_xX_y^{0,+1}$, X = F, Cl, Br; $x + y = 1$–4). The geometries are optimized at B3LYP/6-31+G(2df,p) level. The adiabatic ionization energiess (IE_as), relative energetics of cations, proton affinities (PAs) of silanes, and the enthalpies of formation are predicted using G3(CC) model chemistry. Non-classical ion complex structures are found for hydrogenated cations and transition states connecting classical and non-classical structures are also located. The most stable cations for silylene and silyl radicals have their classical divalent and trivalent structures, and those for silanes have non-classical structures except for SiH_3Br^+ and $SiH_2Br_2^+$. The non-classical structures for halosilane cations imply difficulty in experimentally measurement of the adiabatic ionization energies using photoionization or photoelectron studies. For SiH_3X, SiH_2X_2, and $SiHX_3$, the G3(CC) adiabatic IE_as to classical ionic structures closest to their neutrals agree better with the photoelectron spectroscopic measurements. The transition states between classical and non-classical structures also hamper the photoionization determination of the appearance energies for silylene cations from silanes. The G3(CC) results for $SiH_x^{0,+1}$ agree excellently with the photoionization mass spectrometric study, and the results for fluorinated and chlorinated species also agree with the previous theoretical predictions at correlation levels from BAC-MP4 to CCSD(T)/CBS. The predicted enthalpy differences between SiH_2Cl^+, $SiHCl_2^+$, and $SiCl_3^+$ are also in accordance with previous kinetics study. The G3(CC) results show large discrepancies to the collision-induced charge transfer and/or dissociation reactions involving SiF_x^+ and $SiCl_x^+$ ions, for which the G3(CC) enthalpies of formation are also significantly differed from the previous theoretical predictions, especially on SiF_x^+ ($x = 2$–4). The G3(CC) IE_a and PA of SiF_4 are significantly different from previous experimental and theoretical studies; however, they are supported by current benchmark calculations at level of CCSD(T)/CBS + core-valence correction.

1. Introduction

Halogenated silanes, free radicals, and cations are of interest because of their importance in chemical vapor deposition and surface etching of silicon-containing semiconductor materials. The free radicals and cations play important roles and have been detected in these processes, especially in radio frequency (RF) or plasma-enhanced deposition and etching processes where free radicals and cations have been detected [1–13]. Information on structure and thermodynamics of the silanes, radicals, and cations would provide useful guidelines for selection of processing conditions [9,14]. The ionic silicon species are also of great interest in structural chemistry, where theoretical studies [15–23] on XH_4^+ (X = C, Si, Ge, Sn), $SiH_mF_n^+$, $GeH_mF_n^+$ and $GeH_mCl_n^+$ have revealed large structural distortions to their neutrals. In additional to their occurrence in RF and plasma processes, the ion chemistry is an important method in measuring the bond energies of the neutral species [24].

Because of their importance, there have been many experimental studies on the structure and thermodynamic properties of small silicon-containing compounds. The enthalpies of formation of halogenated silanes have been obtained from the combustion, dissolution, and chemical equilibrium studies, and from empirical linear interpolation estimations. The early results were evaluated and collected in data compilations such as CATCH [25], JANAF-1985 [26], and a review by Walsh [27]. Recently, Hilderbrand et al. [28] reported new enthalpies of formation for $SiCl_x$ and $SiBr_x$ ($x = 1$–3) from the gas-phase equilibrium study.

---

* Corresponding author. Tel.: +86 20 87112900; fax: +86 20 87112906.
E-mail address: wanglm@scut.edu.cn (L. Wang).

1387-3806/$ – see front matter © 2008 Elsevier B.V. All rights reserved.
doi:10.1016/j.ijms.2008.07.004

The experimental studies on the energetics of the ionic species are relatively less. In principle, the enthalpies of formation of cations can be readily obtained from the adiabatic ionization energies (IE_as) and the enthalpies of their neutrals. Unfortunately, it is fairly difficult to obtain the adiabatic ionization energy experimentally, especially for silanes, because of the possible large structural changes from neutrals to cations as being inferred from fluorosilanes [29] and halogermanes [23,30]. The early photoelectron spectroscopic studies measured the vertical IEs instead. Reliable measurements on IE_a were available only to $SiH_x^{0,+1}$ (x = 1–4) from photoionization mass spectrometry study by Berkowitz et al. [31]. There were also reports on IE_a(SiX, X = F,Cl,Br) from photoionization efficiency spectroscopy or VUV spectroscopy of Rydberg states [32–37].

Direct determinations of the enthalpies of formation for cations have been performed on SiH_x^+ [38,39], SiF_x^+ [40–42], and $SiCl_x^+$ [43,44] from collision-induced dissociation and/or charge-transfer studies. Adiabatic IE_as were derived from the energy differences between neutrals and cations, or *vice versa*. In these studies, neither the enthalpies of formation for $SiF_x^{0,+1}$ or $SiCl_x^{0,+1}$ nor the adiabatic IE_as was well defined, and the results carries large uncertainties. Another ion-chemistry study by Murthy and Beauchamp measured the enthalpy difference between SiH_2Cl^+, $SiHCl_2^+$, and $SiCl_3^+$ [45,46]. Large discrepancy exists between experiments for these radicals and cations, e.g., $\Delta_f H^\circ_{298\,K}$ ($SiCl_3$) of -334.7 ± 8.4, -390.4 ± 16.7, and $\geq -351.5 \pm 8.4$ kJ/mol have been reported by Walsh [27], JANAF-1985 [26], and Hilderbrand et al. [28].

With limited experimental studies, quantum chemistry calculations have been used to predict the enthalpies of formation of fluorinated and chlorinated silanes and free radicals [17,29,47–59] and of cations $SiH_xF_y^+$, SiF_x^+, and $SiCl_x^+$ [29,51,53–55,60,61], while none on brominated species. Theoretical studies have found large discrepancies to as well as occasional agreement with the experimental results. On the other hand, agreements between theoretical predictions at levels from BAC-MP4 to Gaussian-3 model chemistry are reasonable. The purpose of present systematic quantum chemistry study on halogenated silanes, radicals, and cations is to predict several quantities pertaining to ion chemistry, including structure, the adiabatic ionization energy, the proton affinity (PA), and the enthalpy of formation, etc. The potential energy surfaces of cations were also explored on the interest of appearance energy of ion fragment and reaction kinetics. The results were compared with and were used to assess the reliability of the previous experimental measurements. Calculations have employed the Gaussian-3 (G3) model chemistry [62–64], and all density functional and molecular orbital calculations were carried out using Gaussian 03 suite of programs [65].

2. Computational details

The geometries are optimized at B3LYP/6-31+G(2df,p) level and the electronic energies are evaluated with the G3 model chemistry [62–64], in which QCISD(T) is replaced by CCSD(T). Transition states are confirmed by the visualization of the displacement vector of the vibrational mode with imaginary frequency or following the intrinsic reaction coordinates for transition state from SiH_3^+ to $SiH^+–H_2$. No relativistic effects are included except the spin–orbit corrections, which are obtained from spectroscopic data [66] and applied to atomic and diatomic species only. The spin–orbit interaction is negligible for other nonlinear polyatomic species. The calculation level closely resembles the G3(CC)//B2df model chemistry (the same high-level correction parameters are used as $A = 6.688$, $B = 3.007$, $C = 6.763$, $D = 1.107$ mHartree) [64], and is denoted as G3(CC) here. For silylene radicals and transition states of silyl cations, unrestricted wavefunctions are used for post-Hartree–Fock calculations whenever RHF-wavefunction instability is found. The newly developed G3X/G4 method is not used because of the over-correction for fluorinated species in extending the basis set from G3Large to G3ExtraLarge at Hartree–Fock level, e.g., $\Delta E(\text{HF}) = E(\text{HF/G3ExtraLarge}) - E(\text{HF/G3Large})$ is -5.77 mHartree for SiF_4, -1.88 mHartree for $SiCl_4$, and -2.25 mHartree for $SiBr_4$. Similar effect has been observed in GeF_4, where ΔE(HF) for GeF_4 is significantly larger than those for $GeCl_4$ and $Ge(OH)_4$ [23].

The enthalpies of formation of the neutrals are obtained directly from the G3 atomization energies. For SiX, thermal correction due to Λ-doublet is also included. The enthalpies of formation of cation M^+ are obtained using the following equation:

$$\Delta_f H^\circ_{0\,K}(M^+) = \text{IEa}(M) + \Delta_f H^\circ_{0\,K}(M)$$

$$\Delta_f H^\circ_{298\,K}(M^+) = \Delta_f H^\circ_{0\,K}(M^+) + (H^T - H^0)_{M^+} - \sum_{\text{Element}} (H^T - H^0)_{\text{Std}}$$

where $(H^T - H^0)_{M+}$ and $(H^T - H^0)_{\text{Std}}$ are the thermal corrections to cation and the elements at their standard states. The “Ion Convention” for $\Delta_f H^\circ_{298\,K}(M^+)$ is adopted here. Note that the “Electron Convention” has been used in previous experimental and theoretical predictions and in JANAF table; therefore their values at 298 K will be lowered by 6.2 kJ/mol when compared with our G3(CC) ones.

Note that in the prediction of the enthalpies of formation, the uncertainty of $\Delta_f H^\circ_{0\,K}$ (Si, g) = 446.0 ± 8 kJ/mol will be transferred to $\Delta_f H^\circ_{0\,K}$ of other species, albeit the uncertainties should be less than 8 kJ/mol. The uncertainties for ionization energies and proton affinities are expected to be similar to that of G3 method, e.g., ∼5 kJ/mol (0.05 eV), and being slightly large for transition barriers. The charges and orbital interactions are analyzed using natural bond orbital package NBO 3.0 as implemented in Gaussian 03 [67].

3. Results and discussion

The geometries are optimized at B3LYP/6-31+G(2df,p) level, and the harmonic vibrational frequencies are evaluated at the same level (Tables S1–S3). Similar to our previous studies on germanium system [23,30], B3LYP tends to predict slightly longer bond lengths than MP2, CCSD(T), and experiments, e.g., B3LYP r_e(Si–F) and r_e(Si–Cl) of 1.630 and 2.092 Å are longer than those of 1.601 and 2.058 Å by experiments [66] and of 1.613 and 2.074 Å by CCSD(T)/aug-cc-pVQZ (AVQZ) [51,53], respectively. For SiF^+, $SiCl^+$, and $SiBr^+$, the B3LYP bond lengths of 1.551, 1.972, and 2.129 Å are longer than the experimental values of 1.526, 1.944, and 2.129 Å [68–70]. For SiF^+, SiF_2^+, and SiF_3^+, B3LYP ones of 1.551, 1.547, and 1.527 Å are also longer than RCCSD(T)/AVQZ of 1.538, 1.534, and 1.520 Å [53]. The small differences in B3LYP geometries result in small G3(CC) energy changes, e.g., G3(CC) energy for SiF_3^+ at CCSD(T)/AVQZ geometry is lower by 1.4 kJ/mol than that at the B3LYP one. Similar effect has also been observed for Ge-system where MP2 structures are slightly more stable [30]. B3LYP method also tends to underestimate the vibrational frequencies for Si–F/Cl/Br stretching modes and to overestimate the ones for Si–H stretching modes, e.g., the B3LYP values of 2126, 993 and 651 cm^{-1}, *vs* the experimental ones of 2041.8, 1050.7, and 678.2 cm^{-1} for SiH^+ [71], SiF^+ [68], and $SiCl^+$ [69], respectively. The B3LYP classical and non-classical structures of $[SiHF]^+$, $[SiH_2F]^+$, and $[SiHF_2]^+$ are also in good agreement with the MP2(Full)/6-311G(d,p) and CCSD(T,Full)/cc-pVTZ ones [22], even though the B3LYP bond lengths are again longer than the MP2 and CCSD(T) ones.

3.1. Ionization energies of SiX (X = H, F, Cl, and Br) (Fig. 1, Table 1)

Ionization removes the unpaired p-electron in Si(^{3}P) and SiX. The G3(CC) IE of 8.12 eV for Si-atom agrees excellently with the experimental value of 8.15 eV [66]. From Si(^{3}P) to SiH, the unpaired p-orbital is perturbed slightly, resulting in a small change of IE from Si-atom (8.12 eV) to SiH (7.94 eV by G3). In SiF, SiCl, and SiBr radicals and cations, the strong orbital interaction between the half-filled or empty p-orbitals of Si-atom and the doubly occupied p-orbital of F/Cl/Br-atom leads to reduced IEs for SiF (7.41 eV), SiCl (7.34 eV), and SiBr (7.33 eV, Table 1). Ionization removes one electron almost exclusively from Si-atom, e.g., NBO charges of 0.75*e* on Si of SiF and 1.73*e* of SiF$^+$; while the strong orbital interaction transfers partial charges from Cl/Br to Si-atom in SiCl$^+$/SiBr$^+$, e.g., NBO charges of 0.48*e* on Si of SiBr and 1.29*e* of SiBr$^+$. The stronger orbital interactions in cations result in significantly shortened bond lengths and increased vibrational frequencies from SiX to SiX$^+$ and minor changes from SiH to SiH$^+$ (1.534–1.520 Å and 2015–2126 cm^{-1}) where no such orbital interaction exists.

The G3(CC) IE$_a$(SiH) of 7.94 eV agrees with the direct photoionization determination of 7.91 ± 0.01 eV [31] and the indirect determination of 7.89 ± 0.01 eV from the enthalpies of formation of SiH$^+$ and SiH [38]. Agreement with the latter is fortuitous since the G3(CC) enthalpies of formation for SiH and SiH$^+$ are 363.0 and 1129.1 kJ/mol at 298 K, being almost equally lower than the experimental values of 376.6 and 1145.6 kJ/mol. The G3(CC) value agrees also with the MP4/6-31G(d,p) prediction of 7.90 eV using isogyric reaction [29].

The Armentrout group has reported adiabatic IE$_a$s for SiF and SiCl from the measured $\Delta_f H^\circ$ of SiF$^+$ and SiCl$^+$. The results were dubious because of the large uncertainties and discrepancies between the measurements. Two IEs each were reported for SiF (7.54 ± 0.16 eV [40] or 7.08 ± 0.10 eV [41]) and SiCl (7.44 ± 0.40 eV [43] and 6.79 ± 0.24 eV [44]). Alternatively, IE$_a$(SiF) of 7.31 ± 0.02 eV from VUV Rydberg spectra [32] was supported by theoretical predictions of 7.21 eV at MP4/6-31G(d,p) level [29], 7.36 eV at CCSD(T)/CBS level [54], and 7.41 eV at G3(CC) level. For IE$_a$(SiCl), Bosser et al. [33] have estimated value of 6.82 eV from only two Rydberg states, and later revised it to 7.368 eV with more Rydberg states [34]. Using mass-selected photoionization efficiency spectroscopy, Marijnissen et al. obtained a much precise value of 7.3296 ± 0.0014 eV [35], which is supported by our G3(CC) prediction of 7.34 eV and by previous CCSD(T)/aug-cc-pVQZ prediction of 7.30 eV [51]. For SiBr, Bosser et al. [33] and Kuznetsova et al. [37] reported IE$_a$ of 6.67 and 7.3 eV from Rydberg spectroscopy. The large error in IE$_a$(SiCl) by Bosser et al. disregards their reliability on IE$_a$(SiBr), while G3(CC) prediction of 7.33 eV supports the value by Kuznetsova et al.

3.2. Ionization energies of SiH$_x$X$_y$ and potential energy surfaces of [SiH$_x$X$_y$]$^+$ (X = F, Cl, Br, x + y = 2) (Figs. 1–3, Table 1)

Ground states of silylene radicals are singlet, even though RHF-wavefunction instability is found for these radicals except for SiF$_2$. Ion complex structures Si$^+$–XH, being located here at B3LYP level, agree closely with the previous ones at MP2(Full)/6-311G(d,p) and CCSD(T,Full)/cc-pVTZ levels [22]. Unlike [GeH$_2$]$^+$, [GeHF]$^+$ and [GeHCl]$^+$, where the most stable structures are ion complexes as Ge$^+$–H$_2$, Ge$^+$–FH, and Ge$^+$–ClH [23], the most stable silylene cations have their normal divalent structures, due primarily to the stronger Si–H bonds than Ge–H ones. At G3(CC) level, the adiabatic IE$_a$s of silylenes increase rapidly with fluorination and much slower with chlorination and bromination. IE$_a$(SiHBr) is even smaller than IE$_a$(SiH$_2$).

For IE$_a$(SiH$_2$), Berkowitz et al. [31] suggested two values of 9.15 ± 0.02 or 9.02 ± 0.02 eV and most probably 9.05 eV, which is supported by G3(CC) prediction of 9.09 eV and previous MP4/6-31G(d,p) of 9.06 eV [29]. Berkowitz et al. [31] also observed IE$_a$(^{3}SiH$_2$) = 8.24 ± 0.02 eV, with which our G3(CC) prediction of 8.24 eV agrees. No experimental study was reported on IE$_a$ of SiHF, SiHCl, or SiHBr. For SiHF, Ignacio and Schlegel [29] obtained IE$_a$ = 9.48 eV at MP4/6-31G(d,p) level, which agrees with our G3(CC) value of 9.47 eV. Antoniotti et al. [22] found that SiHF$^+$ is more stable than Si$^+$–FH by 96.7 kJ/mol at CCSD(T,Full)/aug-cc-pVTZ (AVTZ) level, agreeing excellently with our G3(CC) value of 96.9 kJ/mol.

Westwood [72] first reported IE$_a$(SiF$_2$) = 10.78 ± 0.05 eV from photoelectron spectroscopy, and Fisher et al. [41] later obtained 10.84 ± 0.13 eV from charge transfer reaction between Xe and SiF$_2$$^+$. These values are supported by theoretical predictions of 10.77 eV at MP4/6-31G(d,p) level [29], 10.74 eV [54] and 10.81 eV at CCSD(T)/CBS level [60], and 10.91 eV at G3(CC) level. For SiCl$_2$, Fisher and Armentrout [44] obtained IE$_a$ of 9.81 ± 0.10 eV from the measured $\Delta_f H^\circ$ (SiCl$_2$$^+$), being slightly higher than previous G2 prediction of 9.74 eV [51] and current G3(CC) of 9.64 eV. IE(SiCl$_2$) obtained from electron impact ionization (10.93 ± 0.10 eV) [73] and photoelectron spectroscopy (10.35 eV) [74] are obviously too high. There is no direct measurement on IE(SiBr$_2$) but an estimation of 8.5 ± 1.5 eV [75], compared to G3(CC) prediction of 9.33 eV; while the value of 12 ± 1 eV obtained from electron impact ionization [76] was too high.

The lowest fragmentation channel of SiX$_2$$^+$ (X = F, Cl, Br) is SiX$^+$ + X, and dissociations into Si$^+$ + X$_2$ require much higher energies, e.g., 303.3, 198.5, and 157.2 kJ/mol *vs* 811.3, 465.9, and 411.1 kJ/mol. The fragmentation behaviors of SiHX$^+$ are slightly complicated with the existence of low-lying ion complexes Si$^+$–XH. The potential energy surfaces of SiHX$^+$ are shown in Fig. 3. For SiH$_2$$^+$, channel Si$^+$ + H$_2$ is expected to dominate the collision-induced dissociation, being similar to that of GeH$_2$$^+$ [21,23]; while for SiHX$^+$ (X = F, Cl, Br), channels SiX$^+$ + H will be the major ones, being different from those of GeHF$^+$ and GeHCl$^+$, where the ion complex structures Ge$^+$–XH are lower in energy than normal divalent cations and the lowest dissociation channels are Ge$^+$ + HX. The potential energy surfaces show that it is likely to form Si$^+$–H$_2$ and Si$^+$–FH complexes from reactions of Si$^+$ with H$_2$ and HF under low collision energies, and unlikely to form Si$^+$–ClH or Si$^+$–BrH from Si$^+$ + HCl or HBr. Instead, reaction of Si$^+$ with HCl/HBr will uniquely form SiCl$^+$/SiBr$^+$ + H with negative energy barrier.

3.3. Ionization energies of SiH$_x$X$_y$ and potential energy surfaces of [SiH$_x$X$_y$]$^+$ (X = F, Cl, Br, x + y = 3) (Figs. 1, 2 and 4, Table 1)

Silyl radicals are pyramidal, and direct ionization leads to planar trivalent silyl cations. B3LYP also locates the ion complexes SiX$^+$–H$_2$, SiH$^+$–XH, and SiX$^+$–XH as previous MP2 and CCSD(T) do [22]. These ion complexes are energetically less stable than the normal trivalent structures, in contrast to the germyl cations [23]. The relative energies of SiH$^+$–H$_2$ to SiH$_3$$^+$, SiF$^+$–H$_2$ and SiH$^+$–FH to SiH$_2$F$^+$, and SiF$^+$–FH to SiHF$_2$$^+$ were 96.7, 38.9 and 159.0, and 70.7 kJ/mol at CCSD(T,Full)/AVTZ level, being in accordance with 113.8, 28.8 and 159.5, and 71.4 kJ/mol at G3(CC) level.

The G3(CC) adiabatic IE$_a$s for halogenated silyl radicals are listed in Table 1. Experimental measurements were available only to SiH$_3$, SiF$_3$, SiHCl$_2$ and SiCl$_3$ [31,40,44,77], and theoretical studies were limited to fluorosilyls and SiCl$_3$ [29,51,54]. Present G3(CC) represents the first systematic study on this system. G3(CC) calculations show strong effects from F-substitution with increased IE$_a$ from SiH$_2$F (8.12 eV) to SiF$_3$ (9.17 eV), very small effect from Cl-

Table 1
ZPE, G3(CC)/B2df+ (in Hartree), the adiabatic ionization energies, and literature values (in eV)

Neutral	Cations	ZPE	G3(CC)	IE	Literature (experimental)	Literature (theoretical)
Si	Si^+	0.00000	−288.92405	8.12	8.15[a]	
SiH	SiH^+	0.00477	−289.55091	7.94	7.91 ± 0.01[b], 7.89 ± 0.01[c]	7.90[d]
SiF	SiF^+	0.00223	−388.86223	7.41	7.54 ± 0.16[e], 7.08 ± 0.10[f], 7.31 ± 0.02[g]	7.21[d], 7.36[h]
SiCl	$SiCl^+$	0.00146	−749.10824	7.34	6.82[g], 7.44 ± 0.40[i], 6.79 ± 0.24[j], 7.368[k], **7.33**[l]	7.30[m]
SiBr	$SiBr^+$	0.00116	−2862.61218	7.33	6.69[k], 9.0 ± 1.0[n], 7.3[o]	
SiH_2	SiH_2^+	0.01179	−290.13205	9.09	9.05 ± 0.02[b]	9.06[d]
	Si^+–H_2 ($^2B_2$)	0.01162	−290.11421	9.57		
	Si^+–H_2 ($^2B_1$)	0.01167	−290.11087	9.66		
	TS to Si^+–H_2	0.00655	−290.06715			
SiHF	$SiHF^+$	0.00800	−389.40478	9.47		9.48[d]
	Si^+–FH	0.01030	−389.37018	10.47		
	TS to Si^+–FH	0.00489	−389.32625			
SiF_2	SiF_2^+	0.00506	−488.66626	10.91	10.75 ± 0.05[p], 10.84 ± 0.13[f]	10.77[d], 10.74[h], 10.81[q]
SiHCl	$SiHCl^+$	0.00742	−749.65904	9.16		
	Si^+–ClH	0.00796	−749.62907	9.99		
	TS to Si^+–ClH	0.00448	−749.60465			
$SiCl_2$	$SiCl_2^+$	0.00312	−1209.17801	9.64	9.81 ± 0.10[j], 10.93 ± 0.10[r], 10.35[s]	9.74[t]
SiHBr	$SiHBr^+$	0.00709	−2863.16570	9.05		
	Si^+–BrH	0.00717	−2863.13601	9.86		
	TS to Si^+–BrH	0.00447	−2863.11734			
$SiBr_2$	$SiBr_2^+$	0.00234	−5436.19239	9.33	8.5 ± 1.5[u], 12 ± 1[n]	
SiH_3	SiH_3^+	0.02169	−290.78785	8.15	8.01 ± 0.02[b], 8.135[v], 8.14[w]	8.19[d]
	SiH^+–H_2	0.02006	−290.74290	9.33		
	TS to SiH^+–H_2	0.01649	−290.68694			
SiH_2F	SiH_2F^+	0.01790	−390.05924	8.12		8.05[d]
	SiF^+–H_2	0.01445	−390.04482	8.42		
	SiH^+–FH—*cis*	0.01749	−389.99828	9.77		
	SiH^+–FH—*trans*	0.01773	−389.99837	9.78		
	TS to SiH^+–FH	0.01320	−389.93513			
	TS to SiF^+–H_2	0.01341	−389.90793			
$SiHF_2$	$SiHF_2^+$	0.01363	−489.32961	8.43		8.33[d]
	SiF^+–FH—*cis*	0.01330	−489.30304	9.14		
	SiF^+–FH—*trans*	0.01321	−489.30198	9.17		
	TS to SiF^+–FH	0.00918	−489.21594			
SiF_3	SiF_3^+	0.00922	−588.58528	9.17	9.99 ± 0.24[e], 9.03 ± 0.05[f]	9.09[d], 8.98[h]
SiH_2Cl	SiH_2Cl^+	0.01690	−750.30986	7.90	7.66 ± 0.23[x]	
	SiH^+–ClH—*cis*	0.01524	−750.25599	8.36		
	SiH^+–ClH—*trans*	0.01570	−750.25782	9.28		
	$SiCl^+$–H_2	0.01314	−750.28908	9.32		
	TS to SiH^+–ClH	0.01205	−750.20030			
	TS to $SiCl^+$–H_2	0.01254	−750.17718			
$SiHCl_2$	$SiHCl_2^+$	0.01152	−1209.82907	7.81	7.90 ± 0.10[y]	
	$SiCl^+$–ClH—*cis*	0.00987	−1209.79365	8.72		
	$SiCl^+$–ClH—*trans*	0.01002	−1209.79462	8.70		
	TS to $SiCl^+$–ClH	0.00718	−1209.72370			
$SiCl_3$	$SiCl_3^+$	0.00566	−1669.34297	7.85	7.65 ± 0.15[j], 8.05 ± 0.10[y]	7.84[t]
SiH_2Br	SiH_2Br^+	0.01643	−2863.81444	7.83		
	SiH^+–BrH—*cis*	0.01446	−2863.76242	8.32		
	SiH^+–BrH—*trans*	0.01476	−2863.76446	9.19		
	$SiBr^+$–H_2	0.01271	−2863.79269	9.14		
	TS to SiH^+–BrH	0.01134	−2863.71245			
	TS to $SiBr^+$–H_2	0.01206	−2863.68891			
$SiHBr_2$	$SiHBr_2^+$	0.01057	−5436.83752	7.67		
	$SiBr^+$–BrH—*cis*	0.00899	−5436.80111	8.62		
	$SiBr^+$–BrH—*trans*	0.00918	−5436.80242	8.59		
	TS to $SiBr^+$-BrH	0.00615	−5436.74029			
$SiBr_3$	$SiBr_3^+$	0.00420	−8009.85658	7.63		

Values are obtained from: [a]JANAF table [94]; [b]photoionization [31]; [c]Ion chemistry [38]; [d]BAC-MP4/6-31G(d,p) [29]; [e]Ion chemistry [40]; [f]Ion chemistry [41]; [g]Rydberg series [32]; [h]CCSD(T)/CBS [54]; [i]Ion chemistry [43]; [j]Ion chemistry [44]; [k]Rydberg series [33]; [l]Photoionization mass spectrometry [35]; [m]CCSD(T)/AVQZ calculation [51]; [n]Electron impact ionization [76]; [o]Rydberg series [37]; [p]Photoelectron spectroscopy [72]; [q]CCSD(T)/CBS [60]; [r]Electron impact ionization [73]; [s]Photoelectron spectroscopy [74]; [t]G2(MP2) calculation [51]; [u]Estimation from photoionization [75]; [v]Rydberg series [36]; [w]Photoelectron spectroscopy [78]; [x]Ion-molecule reaction [45,46]; [y]Estimation from photoelectron spectroscopy [77].

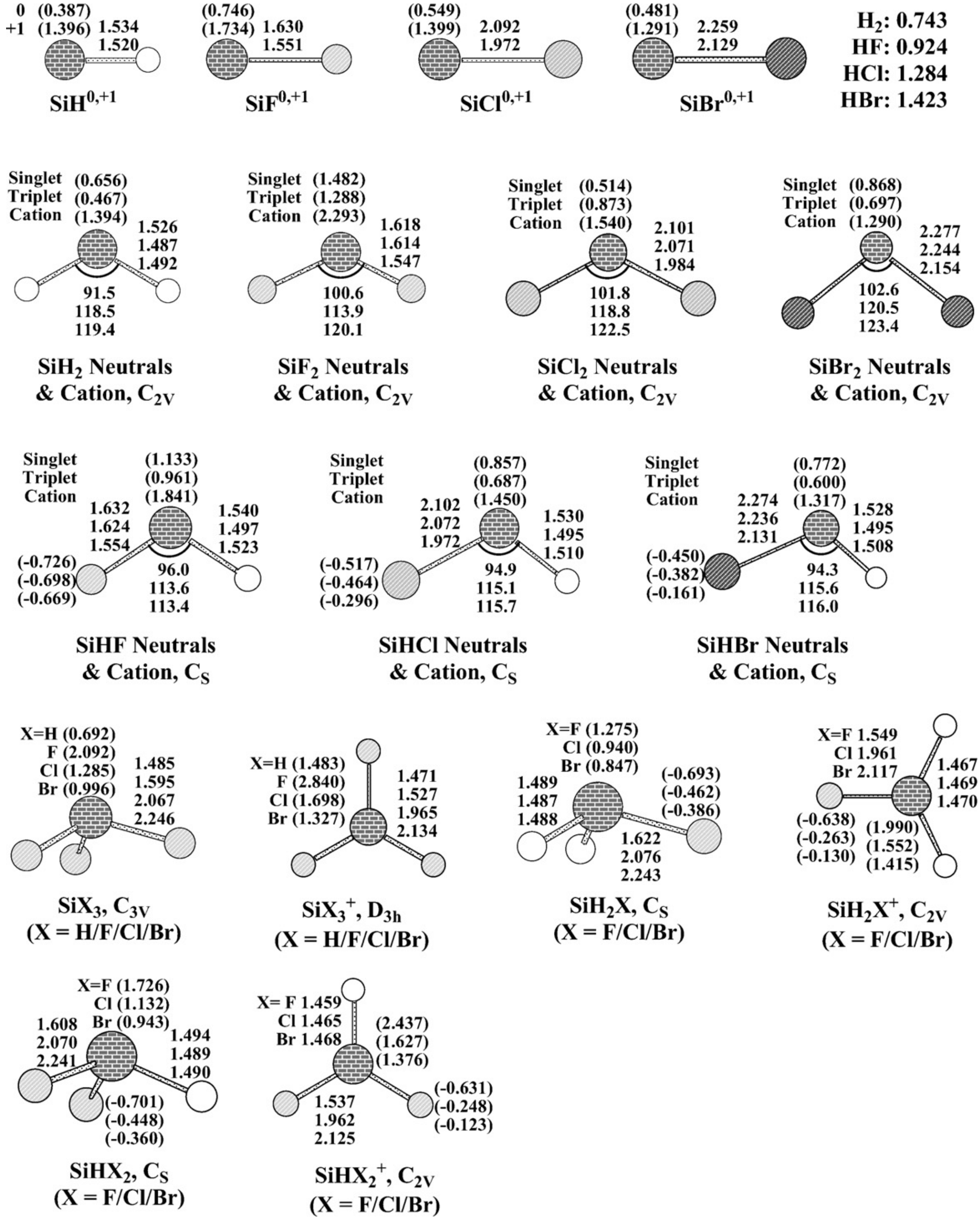

Fig. 1. Geometries of halogenated silyl, silylene, and silylidyne radicals and their most stable cations at B3LYP/6-31+G(2df,p) level (bond lengths in Å and angles in degree) and NBO charges (in parentheses, at CCSD(T)/6-31G(d) level).

substitution with small change of IE$_a$ from SiH_2Cl (7.90 eV) to $SiCl_3$ (7.85 eV), and from Br-substitution with slightly decreased IE$_a$ from SiH_2Br (7.83 eV) to $SiBr_3$ (7.63 eV).

Berkowitz et al. obtained IE$_a$(SiH_3) = 8.01 ± 0.02 eV from photoionization mass spectrometry study of SiH_3 radical [31]. The value is significantly lower than our G3(CC) prediction of 8.15 eV. On the other hand, their measured appearance energy of ≤12.086 eV for SiH_3^+ from SiH_4 is in excellent agreement with our G3(CC) one of 12.065 eV. The G3(CC) IE$_a$ also agrees with the values of 8.135 eV obtained by fitting the Rydberg series [36] and of 8.14 ± 0.01 eV from VUV photoelectron spectroscopy study [78]. The IE$_a$ by Berkowitz et al. [31] is suspected to be too low, and consequently $\Delta_f H^\circ$ (SiH_3) is over-estimated from their $\Delta_f H^\circ$ (SiH_3^+) and IE$_a$(SiH_3).

Weber and Armentrout reported IE$_a$(SiF_3) = 9.99 ± 0.24 eV from $\Delta(\Delta_f H^\circ)$ of SiF_3^+ and SiF_3 [40]. Later, Fisher et al. [41] disregarded this result because an erroneous $\Delta_f H^\circ$ (SiF_3) was used there, and reported another IE$_a$ = 9.03 ± 0.05 eV from the measured thresholds for $SiF_3^+ + M \rightarrow M^+ + SiF_3$ (M = Xe, NO). The latter is supported by the CCSD(T)/CBS prediction of 8.98 eV [54] and MP4/6-31G(d,p) of 9.09 eV [29], while being lower than G3(CC) of 9.17 eV. The IE$_a$ for fluorosilyl radicals from MP4/6-31G(d,p) predictions are found to

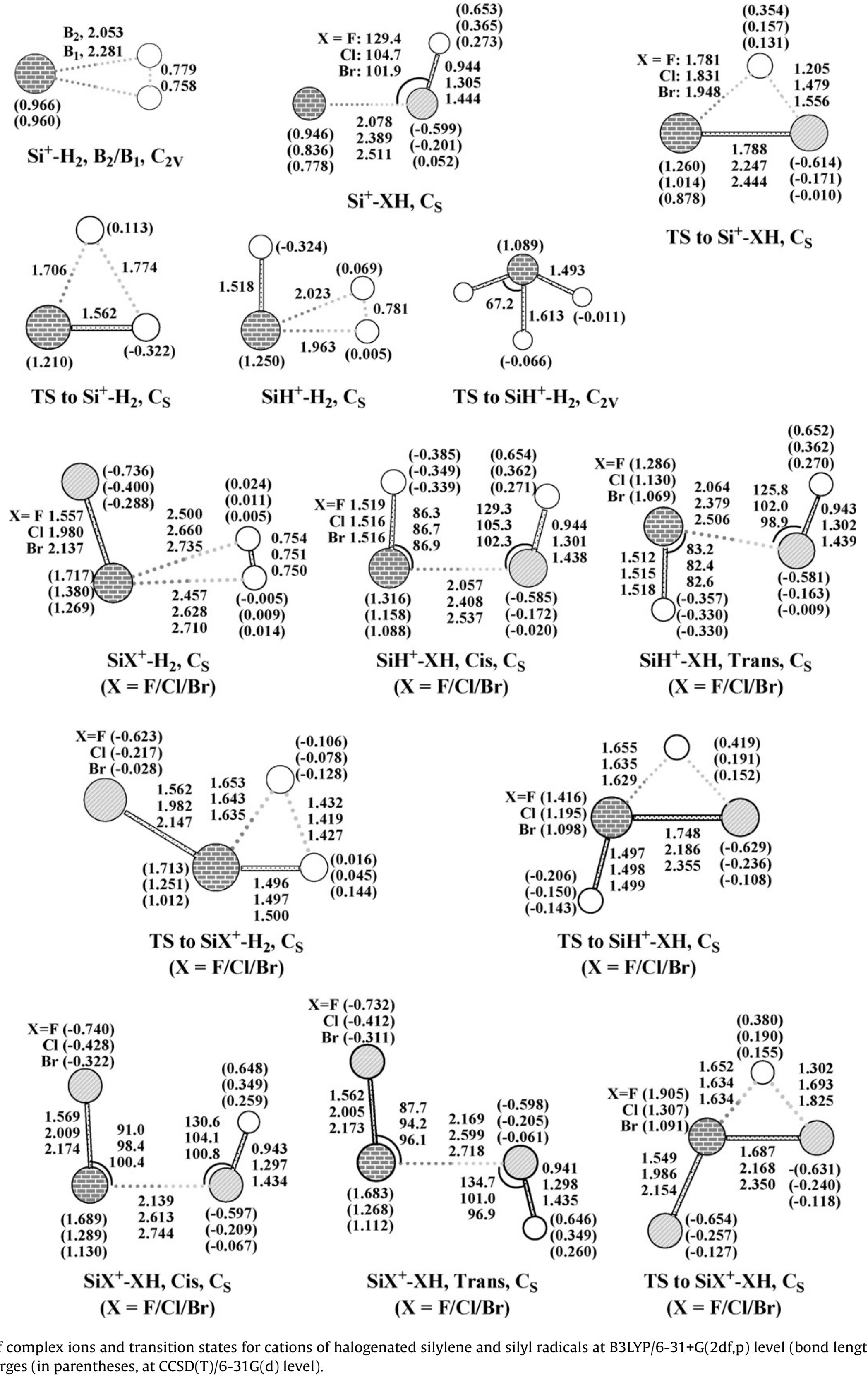

Fig. 2. Geometries of complex ions and transition states for cations of halogenated silylene and silyl radicals at B3LYP/6-31+G(2df,p) level (bond lengths in Å and angles in degree) and NBO charges (in parentheses, at CCSD(T)/6-31G(d) level).

be systematically lower than the G3(CC) ones, e.g., 8.05 and 8.33 eV *vs* 8.12 and 8.43 eV for SiH_2F and $SiHF_2$, respectively.

Fisher and Armentrout [44] reported an $IE_a(SiCl_3) = 7.65 \pm 0.15$ eV from the measured $\Delta(\Delta_f H^\circ)$ of $SiCl_3$ and $SiCl_3^+$. Dyke et al. [77] also reported a value of 8.05 ± 0.10 eV from $IE_{Expt} - \Delta(IE_{MP2})$, where IE_{Expt} was the experimental vertical IE from photoelectron spectroscopy and $\Delta(IE_{MP2})$ was difference between vertical and adiabatic IE_a at MP2/6-31G(d,p) level.

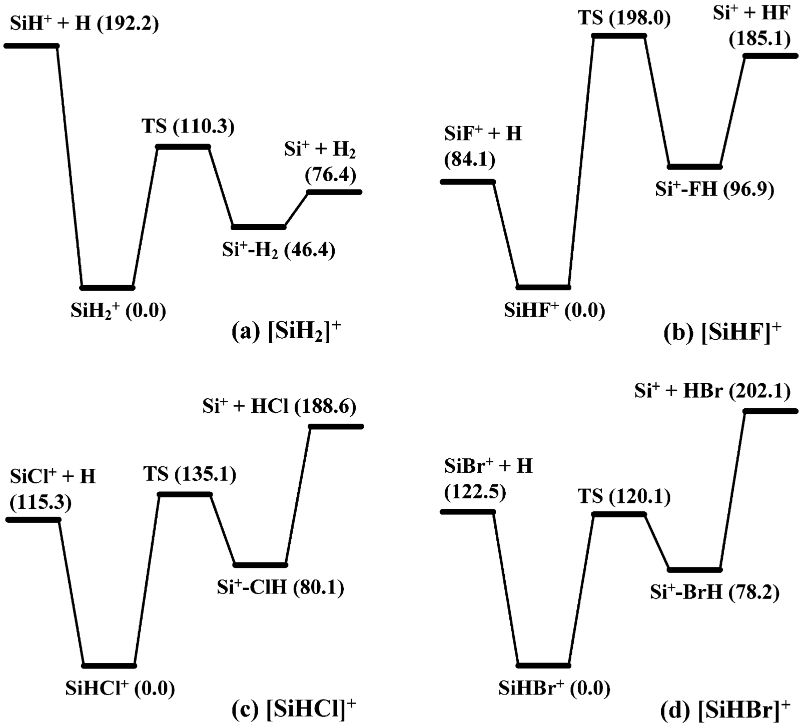

Fig. 3. Potential energy surfaces of $[SiHX]^+$ cations (X = H, F, Cl, Br; relative energies in parentheses are in kJ/mol).

The correction $\Delta(IE_{MP2})$ was rather rough and unlikely valid. Both $IE_a(SiCl_3)$ differ significantly from our G3(CC) prediction of 7.85 eV and previous G2(MP2) of 7.84 eV [51]. Neither the $IE_a(SiHCl_2) = 7.90 \pm 0.10$ eV by Dyke et al. [77] is reliable, even though it agrees accidentally with our G3(CC) of 7.81 eV. Murthy and Beauchamp [45,46] reported an $IE_a(SiH_2Cl) = 7.66 \pm 0.23$ eV using $\Delta_f H^\circ$ (SiH_2Cl^+) obtained from ion–molecule reaction kinetics and $\Delta_f H^\circ$ (SiH_2Cl) from BAC-MP4 prediction [48], being lower than G3(CC) value of 7.90 eV.

The potential energy surfaces of silyl cations are displayed in Fig. 4. For decompositions of SiH_2X^+ and $SiHX_2^+$, the channels with the lowest endothermicity are $SiH^+ + HX$ and $SiX^+ + HX$, respectively, while the breakages of $SiHX^+$–H and SiX_2^+–H bonds are much more endothermic. Transition states between trivalent and complex structures are identified here. The ion complexes are unlikely formed from direct ionization of silyl radicals, while SiH^+–XH and SiX^+–XH might be formed from reactions of SiH^+ and SiX^+ with HX molecule. For SiH_2X^+, the barriers to SiX^+–H_2 are higher than those to SiH^+–XH; therefore $SiH^+ + HX$ will be the dominant decomposition channels under low photon or collision energies, even though they are more endothermic than $SiX^+ + H_2$. Note that in post-HF calculations for theses transition barriers, UHF-wavefunction is required for silyl cations because of the RHF-instability. Thereafter, the barrier heights may be over-predicted.

3.4. Ionization energies of SiH_xX_y and potential energy surfaces of $[SiH_xX_y]^+$ (X = F, Cl, Br, x + y = 4) (Figs. 5–9, Table 2)

Similar to cations of halogenated germane, large structural distortions to their neutrals are expected for cations of halogenated silanes. Experimental adiabatic IE_as were only available for SiH_4 [31] and SiF_4 [42], while values for other species listed on NIST website [66] were exclusively obtained from electron impact ionization and photoelectron spectroscopy, which measure vertical IEs. Theoretical predictions are available to fluorinated and chlorinated silanes [29,51,54,55], especially the IE_a values for fluoro- and chlorosilanes obtained from previous G3 study [55] differ from current G3(CC) ones only slightly, within 0.03 eV except for SiH_2Cl_2, for which G3(CC) value is 0.08 eV lower.

From photoionization mass spectrometry, Berkowitz et al. [31] obtained $IE_a(SiH_4) = 11.00 \pm 0.02$ eV, with which our G3(CC) value of 11.04 eV agrees excellently. Structure of SiH_4^+ has symmetry of Cs point group at B3LYP level and can be viewed as SiH_2^+–H_2 complex (Fig. 5). Similar large structural distortion to the neutral has also been found in $[GeH_4]^+$ and $[SnH_4]^+$ [20,23]. The structural changes are due to spin–orbit coupling and/or the Jahn–Teller effect [79].

HOMOs of SiF_4, $SiCl_4$, and $SiBr_4$ have triple degeneracy. In cations, the spin–orbit interaction and/or Jahn–Teller effect cause a change in molecular shape and the degeneracy is lifted, and the symmetries are reduced to C_{2V} (Fig. 5). The two halogen atoms with less negatively charge experience less repulsion to each other, leading to small XSiX angle of 76.4°, 81.4°, and 81.8°, while the other two atoms open to large XSiX angles of 119.6°, 117.5°, and 117.3° in SiF_4^+, $SiCl_4^+$, and $SiBr_4^+$, respectively. The large structural change leads to difficulty in determining the adiabatic IE in photoionization study because of the small Franck-Condon factors at the ionization onsets. As noticed in previous studies [51,54], the C_S structures of SiF_3^+–F and $SiCl_3^+$–Cl for SiF_4^+ and $SiCl_4^+$ found at HF and MP2 level converge to C_{2V} structures at B3LYP/6-31+G(2df,p) level. Attempt for a C_S structure for $SiBr_4^+$ at B3LYP level also leads to C_{2V} structure. For SiF_4^+ at MP2 level, the C_S structure is *ca.* 4.6 kJ/mol lower in energy than the C_{2V} one at CCSD(T)/CBS level [54].

Several photoelectron spectroscopy studies have reported closely agreed vertical IE around 16.46 eV for SiF_4 [80–83], which is supported by current G3(CC) prediction of 16.54 eV. On the other hand, the reported $IE_a(SiF_4)$ were rather diverse. Kickel et al. [42] found that early studies obtained $IE_a(SiF_4)$ in the range of 15.19–16.1 eV [66], and suggested another $IE_a(SiF_4) = 15.29 \pm 0.08$ eV from the measured threshold for charge transfer reaction $O^+/N^+ + SiF_4 \rightarrow O/N + SiF_4^+$. This value is consid-

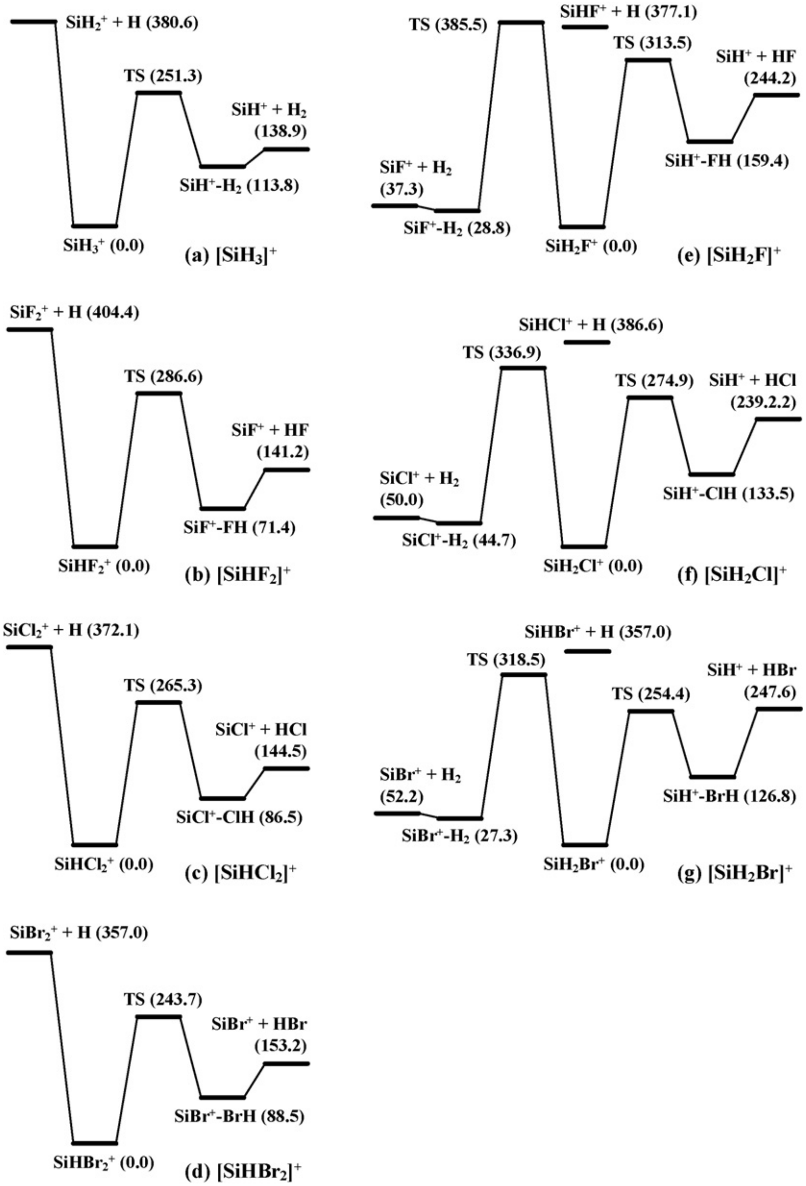

Fig. 4. Potential energy surfaces of $[SiH_2X]^+$ and $[SiHX_2]^+$ cations (X = H, F, Cl, Br; relative energies in parentheses are in kJ/mol).

ered to be the best so far, and has received support from theoretical predictions of 15.34 eV at MP4/6-31G(d,p) level [29] and of 15.34 eV at CCSD(T)/AVTZ + MP2/CBS level (converted from their enthalpies of formation at 298 K using current B3LYP thermal corrections) [54]. However, Chien et al. [55] pointed out that the agreement at MP4/6-31G(d,p) level might be fortuitous because MP4 calculations with larger basis set yield much different values. For $SiCl_4$, IE_a of 11.79 ± 0.01 eV [81] from photoelectron spectrum and 11.7 ± 0.3 eV [84] from electron impact ionization have been reported, and for $SiBr_4$, 10.62 ± 0.04 eV [75] from photoionization mass spectromet-

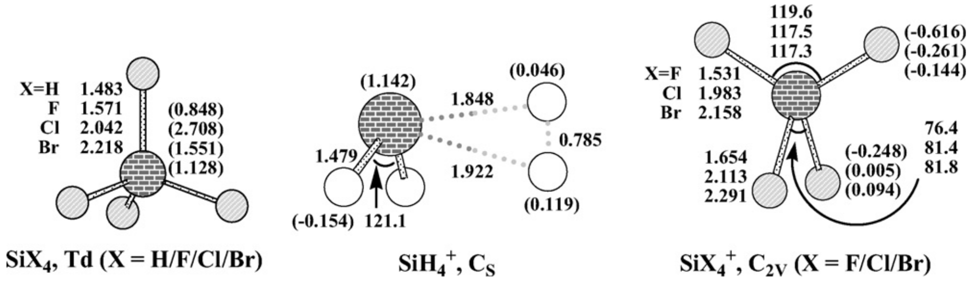

Fig. 5. Geometries of $[SiX_4]^{0,+1}$ (X = H, F, Cl, Br) at B3LYP/6-31+G(2df,p) level (bond lengths in Å and angles in degree) and NBO charges (in parentheses, at CCSD(T)/6-31G(d) level).

Table 2
ZPE, G3(CC)/B2df+ (in Hartree), the adiabatic ionization energies, and literature values (in eV)

	Cations		ZPE	G3(CC)	IE[a]	Literature (experimental)	Literature (theoretical)
SiH_4	$SiH_2{}^+–H_2$	C_S	0.02819	−291.33278	**11.04**	11.00 ± 0.02[b]	11.17[c], 11.05[d]
SiH_3F	SiH_3F^+	C_S	0.02199	−390.57709	*11.81*	12.58[e], 12.6 ± 0.1[f]	12.04[c]
	$SiHF^+–H_2$	C_1	0.02301	−390.59646	**11.31**	11.92[f]	11.48[c]
	$SiH_2{}^+–FH$	C_1	0.02573	−390.58864	11.59		12.49,[c] 11.59[d]
	TS to $SiHF^+–H_2$	C_1	0.02153	−390.56966			
	TS to $SiH_2{}^+–FH$	C_S	0.02162	−390.53900			
SiH_2F_2	$SiH_2F_2{}^+$	C_{2V}	0.01676	−489.84469	*12.27*	12.85[e]	12.9 ± 0.1[f], 12.45[c]
	$SiF_2{}^+–H_2$	C_S	0.01865	−489.86061	**11.89**		12.15[c]
	$SiHF^+–FH$	C_1	0.02102	−489.85943	11.99		11.87[c], 11.98[d]
	TS to $SiF_2{}^+–H_2$	C_S	0.01581	−489.82277			
	TS to $SiHF^+–FH$	C_1	0.01716	−489.80684			
$SiHF_3$	$SiHF_3{}^+$	C_{3V}	0.01231	−589.10679	*13.03*	14.48 ± 0.02[g]	13.24[c]
	$SiF_2{}^+–FH$	C_1	0.01682	−589.12697	**12.61**		12.45[c], 12.58[d]
	TS to $SiF_2{}^+–FH$	C_S	0.01260	−589.07026			
SiF_4	$SiF_4{}^+$	C_{2V}	0.01083	−688.29559	**15.74**	16.46[h], 15.29 ± 0.08[i]	15.34[j], 15.34[c], 15.65[d]
SiH_3Cl	SiH_3Cl^+	C_S	0.02233	−750.83187	*11.40*	11.61[e], 11.65[f], 11.51[k]	
	$SiHCl^+–H_2$	C_1	0.02200	−750.84651	**10.99**		11.03[d]
	$SiH_2{}^+–ClH$	C_1	0.02351	−750.84738	11.01		
	TS to $SiHCl^+–H_2$	C_1	0.02071	−750.82365			
	TS to $SiH_2{}^+–ClH$	C_S	0.02075	−750.81578			
SiH_2Cl_2	$SiH_2Cl_2{}^+$	C_S	0.01549	−1210.34165	*11.53*	11.70[e], 11.64 ± 0.02[f]	
	$SiCl_2{}^+–H_2$	C_S	0.01565	−1210.36111	**11.01**		
	$SiHCl^+–ClH$	C_1	0.01766	−1210.36039	11.08		11.09[d]
	TS to $SiCl_2{}^+–H_2$	C_S	0.01467	−1210.32973			
	TS to $SiHCl^+–ClH$	C_1	0.01528	−1210.32831			
$SiHCl_3$	$SiHCl_3{}^+$	C_{3V}	0.00904	−1669.85534	*11.60*	11.94[e]	
	$SiHCl_3{}^+$	C_S	0.01311	−1669.86366	11.48		
	$SiCl_2{}^+–ClH$	C_1	0.01205	−1669.87450	**11.16**	11.15[d]	11.15[d]
	TS to $SiCl_2{}^+–ClH$	C_S	0.00933	−1669.84018			
$SiCl_4$	$SiCl_4{}^+$	C_{2V}	0.00666	−2129.37566	**11.55**	11.79 ± 0.01[l], 11.7 ± 0.3[m]	11.66[d]
SiH_3Br	SiH_3Br^+	C_S	0.02318	−2864.35609	***10.80***	10.90[e], 10.96 ± 0.02[f]	
	$SiHBr^+–H_2$	C_1	0.02143	−2864.35178	10.87	11.03 ± 0.05[n]	
	$SiH_2{}^+$-BrH	C_1	0.02262	−2864.35391	10.84		
	TS to $SiHBr^+–H_2$	C_1	0.02022	−2864.32969			
	TS to $SiH_2{}^+$-BrH	C_S	0.02010	−2864.32772			
SiH_2Br_2	$SiH_2Br_2{}^+$	C_{2V}	0.01855	−5437.38304	**10.53**	10.92 ± 0.02[f]	
	$SiH_2Br_2{}^+$	C_S	0.01561	−5437.36159	*11.04*		
	$SiBr_2{}^+–H_2$	C_S	0.01418	−5437.37355	10.67		
	$SiHBr^+$-BrH	C_1	0.01674	−5437.37056	10.82		
	TS to $SiBr_2{}^+–H_2$	C_S	0.01381	−5437.34138			
	TS to $SiHBr^+$-BrH	C_1	0.01403	−5437.34446			
$SiHBr_3$	$SiHBr_3{}^+$	C_S	0.00841	−8010.37417	*11.11*		
	$SiBr_2{}^+$-BrH	C_1	0.01053	−8010.38987	**10.74**		
	TS to $SiBr_2{}^+$-BrH	C_S	0.00757	−8010.36146			
$SiBr_4$	$SiBr_4{}^+$	C_{2V}	0.00481	−10583.41381	**10.52**	10.62 ± 0.04[o]	

[a] IEs are calculated from G3(CC) electronic energy differences between cations and neutrals with ZPE corrections. Values in *italics* are for cations with structures closest to their neutrals, and values in **bold** are the adiabatic IE to the ground cation; [b] From photoionization study [31]; [c] Adiabatic IE from isogyric reactions at MP4/6-31G(d,p) level [29]; [d] Adiabatic IE from G3 calculation [55]; [e] Vertical IEs from photoelectron spectroscopy [86]; [f] Vertical IEs from photoelectron spectroscopy [88]; [g] Vertical IE from photoelectron spectroscopy [90]; [h] Vertical IE from photoelectron spectroscopy [80–83]; [i] Adiabatic IE from ion chemistry [42]; [j] Adiabatic IE from CCSD(T)/AVTZ + MP2/CBS [54]; [k] Vertical IE from photoelectron spectroscopy [89]; [l] From photoelectron spectroscopy [81]; [m] From electron impact ionization [84]; [n] From photoelectron spectroscopy [87]; [o] From photoionization mass spectrometry [75].

ric study. These values are slightly higher than our G3(CC) adiabatic IE_as of 11.55 and 10.52 eV for $SiCl_4$ and $SiBr_4$, respectively. The G3(CC) $IE_a(SiCl_4)$ is slightly lower than previous G3 value of 11.66 eV [55] and G2(MP2) of 10.67 eV (with Cs symmetry for $SiCl_4{}^+$) [51].

At B3LYP/6-31+G(2df,p) level, both classical and non-classical structures are identified for cations of SiH_3X, SiH_2X_2, and $SiHX_3$ (Figs. 6–8). The non-classical structures can be viewed as ion complexes between silylene cations and H_2 or HX with a small fraction of positive charge partitioned to H_2 or HX moieties. Previous studies have found this type of structure for cations of fluorinated and chlorinated silanes [29,85] and germanes [23]. The non-classical structures are lower in energy than the classical ones except for $[SiH_3Br]^+$ and $[SiH_2Br_2]^+$. It is again difficult to measure the adiabatic IE_as to the non-classical cations. The measured "adiabatic" or vertical IEs from photoelectron spectroscopy correspond most likely to the classical cationic structure instead.

Symmetries of cations of SiH_3X (X = F, Cl, Br) are reduced due to the spin–orbit interaction and Jahn–Teller effect (Fig. 6). Ion complexes $SiHF^+–H_2$, $SiH_2{}^+–FH$, $SiHCl^+–H_2$, and $SiH_2{}^+–ClH$ are lower in energy than their classical ones, while the three $[SiH_3Br]^+$ structures are within 7 kJ/mol. Photoelectron spectroscopic studies have obtained vertical IEs of 11.61–11.65 eV and 10.96–11.03 eV for SiH_3Cl and SiH_3Br [86–89]. These vertical IEs are close to the predicted vertical IEs of 11.73 and 11.02 eV and slightly higher than the predicted

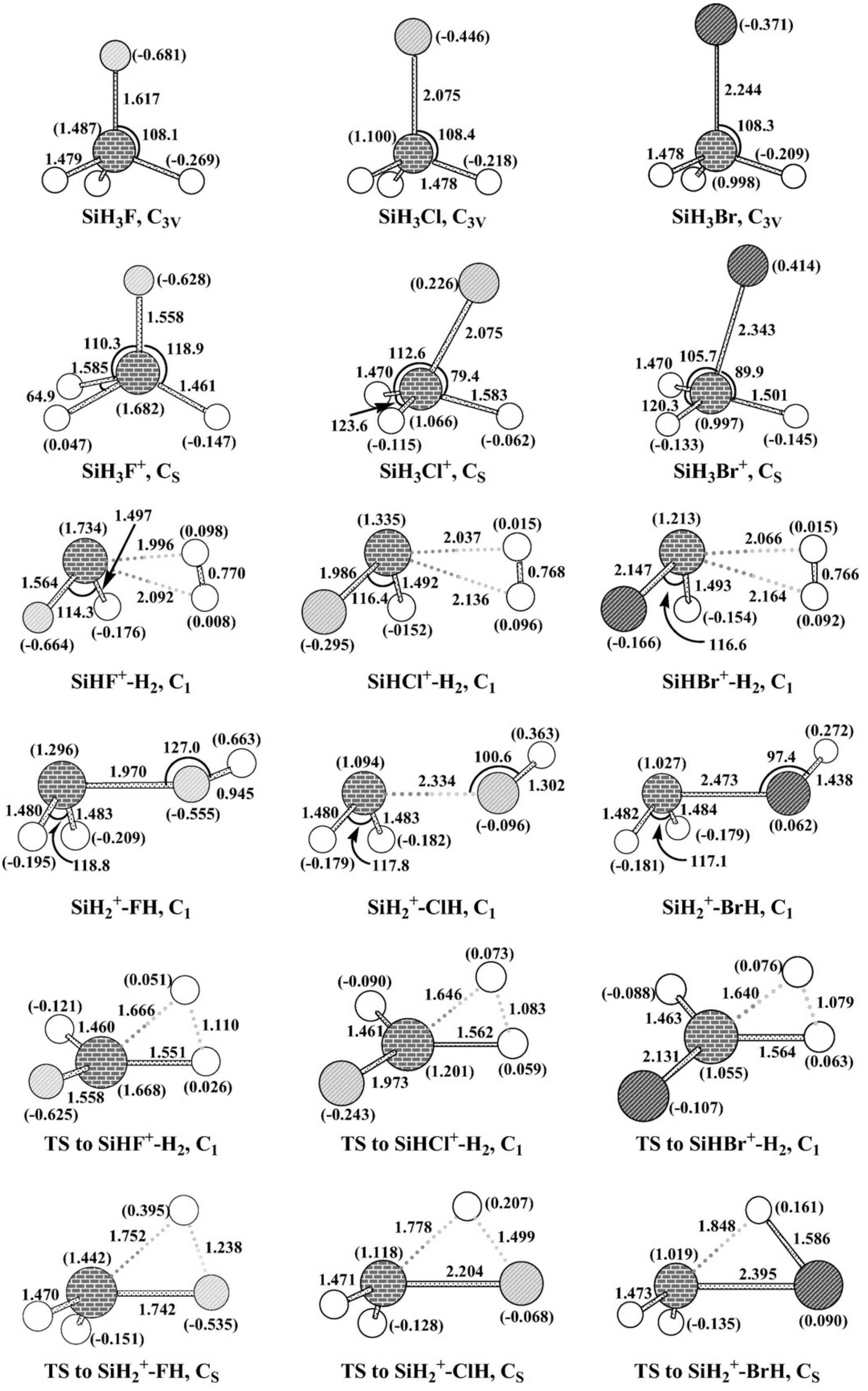

SiH_3F, C_{3V} SiH_3Cl, C_{3V} SiH_3Br, C_{3V}

SiH_3F^+, C_S SiH_3Cl^+, C_S SiH_3Br^+, C_S

$SiHF^+$-H_2, C_1 $SiHCl^+$-H_2, C_1 $SiHBr^+$-H_2, C_1

SiH_2^+-FH, C_1 SiH_2^+-ClH, C_1 SiH_2^+-BrH, C_1

TS to $SiHF^+$-H_2, C_1 TS to $SiHCl^+$-H_2, C_1 TS to $SiHBr^+$-H_2, C_1

TS to SiH_2^+-FH, C_S TS to SiH_2^+-ClH, C_S TS to SiH_2^+-BrH, C_S

Fig. 6. Geometries of $[SiH_3X]^{0,+1}$ (X = F, Cl, Br) at B3LYP/6-31+G(2df,p) level (bond lengths in Å and angles in degree) and NBO charges (in parentheses, at CCSD(T)/6-31G(d) level).

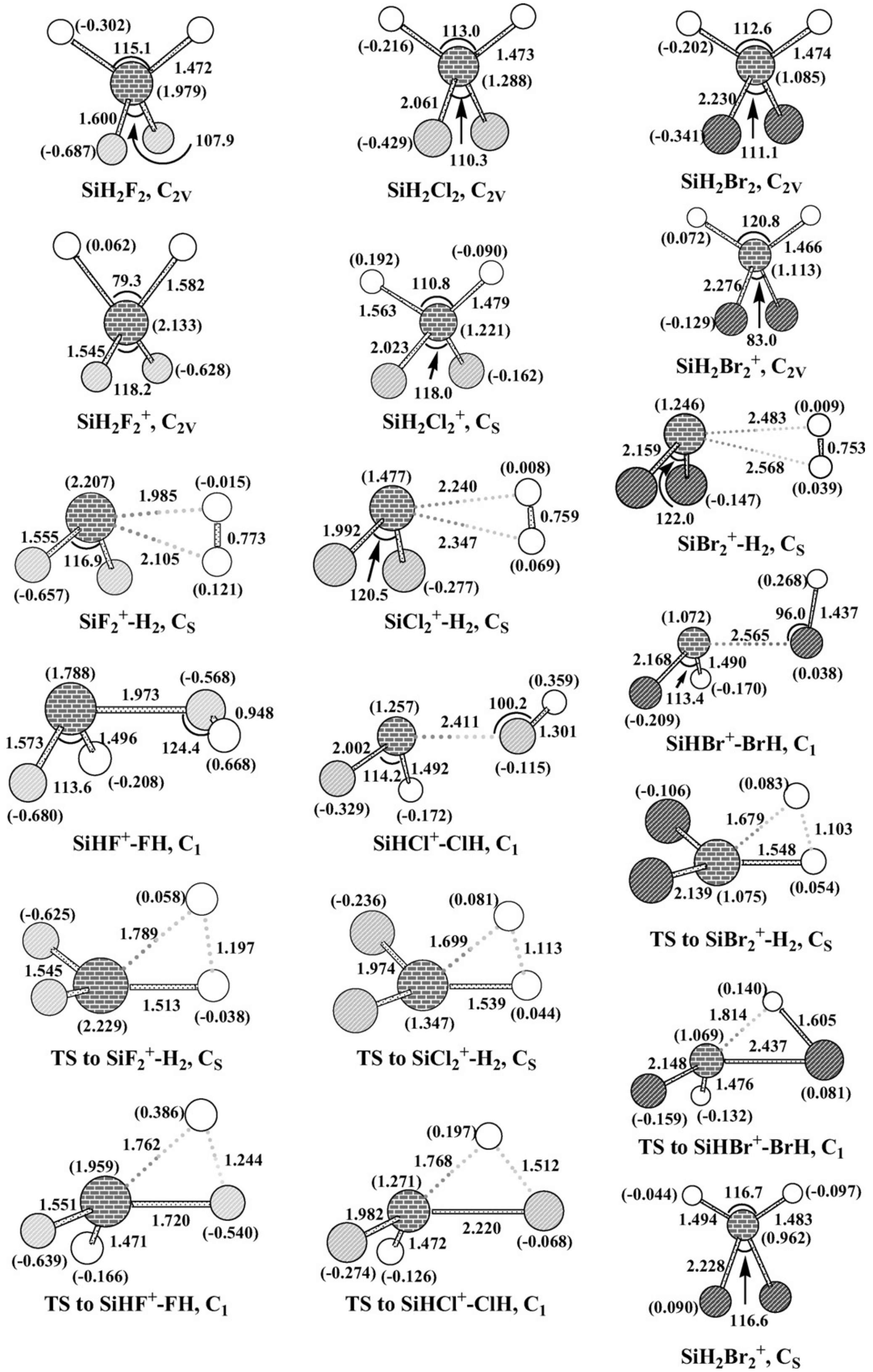

SiH_2F_2, C_{2V}

$SiH_2F_2^+$, C_{2V}

SiF_2^+-H_2, C_S

$SiHF^+$-FH, C_1

TS to SiF_2^+-H_2, C_S

TS to $SiHF^+$-FH, C_1

SiH_2Cl_2, C_{2V}

$SiH_2Cl_2^+$, C_S

$SiCl_2^+$-H_2, C_S

$SiHCl^+$-ClH, C_1

TS to $SiCl_2^+$-H_2, C_S

TS to $SiHCl^+$-ClH, C_1

SiH_2Br_2, C_{2V}

$SiH_2Br_2^+$, C_{2V}

$SiBr_2^+$-H_2, C_S

$SiHBr^+$-BrH, C_1

TS to $SiBr_2^+$-H_2, C_S

TS to $SiHBr^+$-BrH, C_1

$SiH_2Br_2^+$, C_S

Fig. 7. Geometries of $[SiH_2X_2]^{0,+1}$ (X = F, Cl, Br) at B3LYP/6-31+G(2df,p) level (bond lengths in Å and angles in degree) and NBO charges (in parentheses, at CCSD(T)/6-31G(d) level).

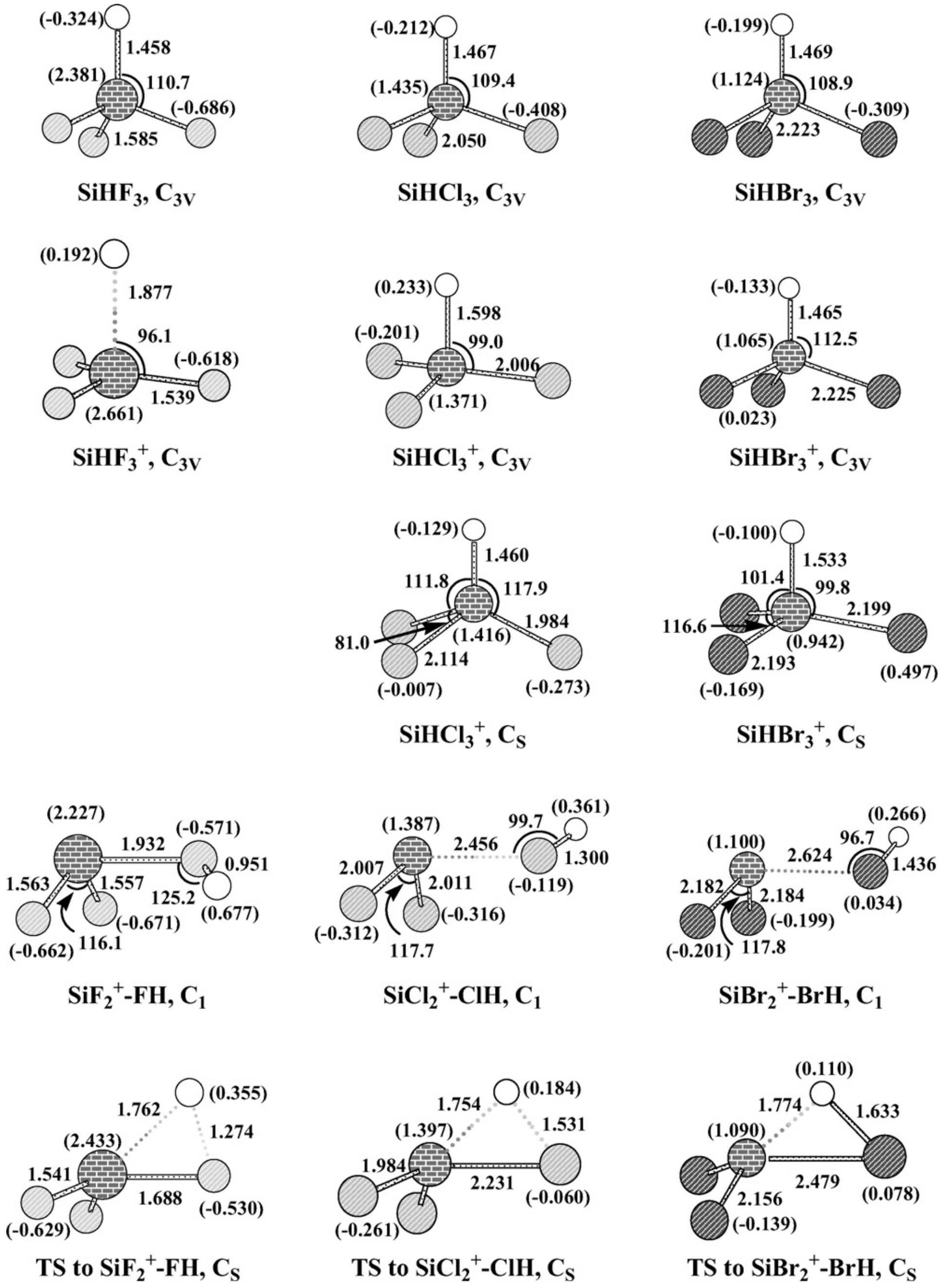

Fig. 8. Geometries of $[SiHX_3]^{0,+1}$ (X = F, Cl, Br) at B3LYP/6-31+G(2df,p) level (bond lengths in Å and angles in degree) and NBO charges (in parentheses, at CCSD(T)/6-31G(d) level).

adiabatic IE_as of 11.40 and 10.80 eV to classical SiH_3Cl^+ and SiH_3Br^+, respectively, at G3(CC) level. For SiH_3Cl, the "true" IE_a is 10.99 eV to $SiHCl^+–H_2$ or 11.01 eV to $SiH_2{}^+–ClH$; while for SiH_3F, the G3(CC) IE_a of 11.81 eV to SiH_3F^+ is much lower than the vertical IE of ∼12.6 eV by photoelectron spectroscopy [86,88].

Three structures are located for $[SiH_2X_2]^+$ cations as $SiX_2{}^+–H_2$, $SiHX^+–XH$, and tetravalent $SiH_2X_2{}^+$ (Fig. 7). The ion complexes are structurally similar across the halogen substitutions, while the structural difference for $SiH_2X_2{}^+$ is interesting. $SiH_2F_2{}^+$ has C_{2V} symmetry with opened FSiF angle to 118.2°, closed HSiH angle to 79.3°, lengthened Si–H bond from 1.472 to 1.582 Å, and shortened Si–F bond from 1.600 to 1.545 Å. $SiH_2Br_2{}^+$-C_{2V} has similar structure with, however, closed BrSiBr angle to 83.0°, opened HSiH angle to 120.8°, shortened Si–H bonds, and lengthened Si–Br bonds. In between, $SiH_2Cl_2{}^+$-C_{2V} structure is a first-order saddle point, and B3LYP instead locates a $SiH_2Cl_2{}^+$-C_S structure which is structurally close to neutral SiH_2Cl_2 and energetically *ca.* 7 kJ/mol below $SiH_2Cl_2{}^+$-C_{2V}. B3LYP also locates a similar $SiH_2Br_2{}^+$-C_S structure being *ca.* 48 kJ/mol above $SiH_2Br_2{}^+$-C_{2V}. The vertical IEs of ∼12.9, ∼11.7, and 10.92 eV have been reported for SiH_2F_2, SiH_2Cl_2, and SiH_2Br_2 [86,88], respectively, using photoelectron spectroscopy technique. The values are close to the predicted vertical IEs of 13.06, 11.71, and 11.10 eV and slightly higher than the predicted adiabatic IE_as of 12.27, 11.53, and 11.04 eV to $SiH_2F_2{}^+$-C_{2V}, $SiH_2Cl_2{}^+$-C_S and $SiH_2Br_2{}^+$-C_S, respectively, at G3(CC) level.

HOMOs of $SiHX_3$ (X = F, Cl, Br) are non-degenerate. The C_{3V} symmetry may possibly be retained in their cations (Fig. 8). At B3LYP/6-31+G(2df,p) level, $SiHF_3{}^+$ and $SiHCl_3{}^+$ with C_{3V} symmetry are indeed local minima, while $SiHBr_3^+$ with C_{3V} symmetry has two imaginary vibrational frequencies and the symmetry needs to be lowered to C_S for a stationary point. For $SiHCl_3^+$, lowering the symmetry to C_S leads to more stable structure in which one HSiCl-angle is open to 117.9° and the other two Cl-atoms are brought close to ClSiCl angle of 81.0°. From $SiHF_3$ to $SiHF_3^+$-C_{3V}, the Si–H bond length stretches from 1.458 to 1.877 Å, Si–F shrinks from 1.585 to 1.539 Å, and SiF_3^+ moiety is close to planar (FSiF = 118.9°). Changes are relatively less from $SiHCl_3$ to $SiHCl_3^+$-C_{3V} and from $SiHBr_3$ to $SiHBr_3^+$-C_{3V} or $SiHBr_3^+$-C_S, e.g., Si–H from 1.467 to 1.598 Å, S–Cl from 2.050 to 2.006 Å, and ClSiCl = 117.6°. Photoelectron spectroscopy studies have obtained vertical IEs of 14.48 ± 0.02 and 11.94 eV for $SiHF_3$ [90] and $SiHCl_3$ [86], respectively. The values are supported by G3(CC) predictions of 14.60 and 12.00 eV. The vertical IE($SiHF_3$) is significantly larger than $IE_a(SiHF_3)$ of 13.03 eV (to $SiHF_3^+$-C_{3V}) because of the large structural changes fro $SiHF_3$ to $SiHF_3^+$-C_{3V}, while the vertical IE($SiHCl_3$) is only slightly higher than $IE_a(SiHCl_3)$ of 11.60 eV to $SiHCl_3^+$-C_{3V} or 11.48 eV to $SiHCl_3^+$-C_S with less structural changes. For cations of $SiHX_3$, SiX_2^+–XH structures are always energetically more stable than the classical ones; however, it is difficult to observe them in photoionization study.

We have also located the transition states between the classical and ion-complex structures for halogenated silane cations, and evaluated their relative energetics at G3(CC) level (Fig. 9). While the appearance energies for silyl cations from dissociative photoionization of silanes are likely equal to their endothermicities, the appearances of silylene cations + H_2/HX are complicated because of the transition barriers between classical and non-classical structures. If the photoionization prompts silanes to their classical cations, the appearance energies for $SiHX^+ + H_2$ and $SiX_2^+ + H_2$ (X = F, Cl, Br) from SiH_3X and SiH_2X_2, $SiH_2^+ + HF$ from SiH_3F, $SiHF^+ + HF$ from SiH_2F_2, and $SiF_2^+ + HF$ from $SiHF_3$ indeed correspond to the transition barriers, while those of $SiH_2^+ + HX$ from SiH_3X, $SiHX^+ + HX$ from SiH_2X_2, and $SiX_2^+ + HX$ from $SiHX_3$ (X = Cl, Br) are equal to their endothermicities because the transition barriers are energetically below these exit channels.

3.5. Proton affinities of silanes (Table 3, Fig. 10)

Proton affinity is one of the important parameters in gas-phase ion-chemistry [24]. The experimental measurements on PAs are available for SiH_4 and SiF_4 only [91,92], and theoretical G3 study on PAs of fluorinated and chlorinated silanes [55]. Fig. 10 shows the structures of protonated silanes, which can be viewed as the complex ions between silyl cations and H_2 or XH (X = F, Cl, Br). For SiH_3X, SiH_2X_2, and $SiHX_3$, protonations at X-atom are relatively more stable except for SiH_3F and SiH_2F_2. The PAs for SiH_3F and SiH_2F_2 given by Chien et al. [55] corresponds to protonations at F-atom. For others, our G3(CC) agrees with G3 within 3 kJ/mol while being systematically higher. For PAs at 298 K, it is necessary to treat one of the low-frequency vibrational modes as hindered or free rotor. The mode corresponds to the torsion mode in complexes with H_2 or the internal rotation around Si–X bond in complexes with HX. Following the suggestion by Nicolaides et al. [93], we have assigned thermal contribution of RT/2 at 298 K to the torsion or internal rotation modes with frequency less than 260 cm^{-1}.

Table 3 lists the calculated PAs and dissociation energies D_0(Silyl$^+$–H_2/HX). For silyl$^+$–H_2, the bonding between silyl$^+$ and H_2 is weak, where the silyl$^+$ moiety is almost planar (summation of three bond angles in the range of 355–399.8°) and the H_2 moiety carries only a small fraction of positive charge. For silyl$^+$–XH, the bond strengths are from 80 to 173 kJ/mol at G3(CC) level, being relatively stronger, and the silyl cations are less planar (summations of the angles in the range of 350–355°).

The calculated G3(CC) PA(SiH_4) = 634.0 kJ/mol falls in the range of 628–653 kJ/mol by Cheng and Tampe from Tandem mass spectroscopy study [91], and agrees with the value of 639.7 kJ/mol listed by Hunter and Lias [94]. For SiF_4, Ling et al. [92] recently obtained PA

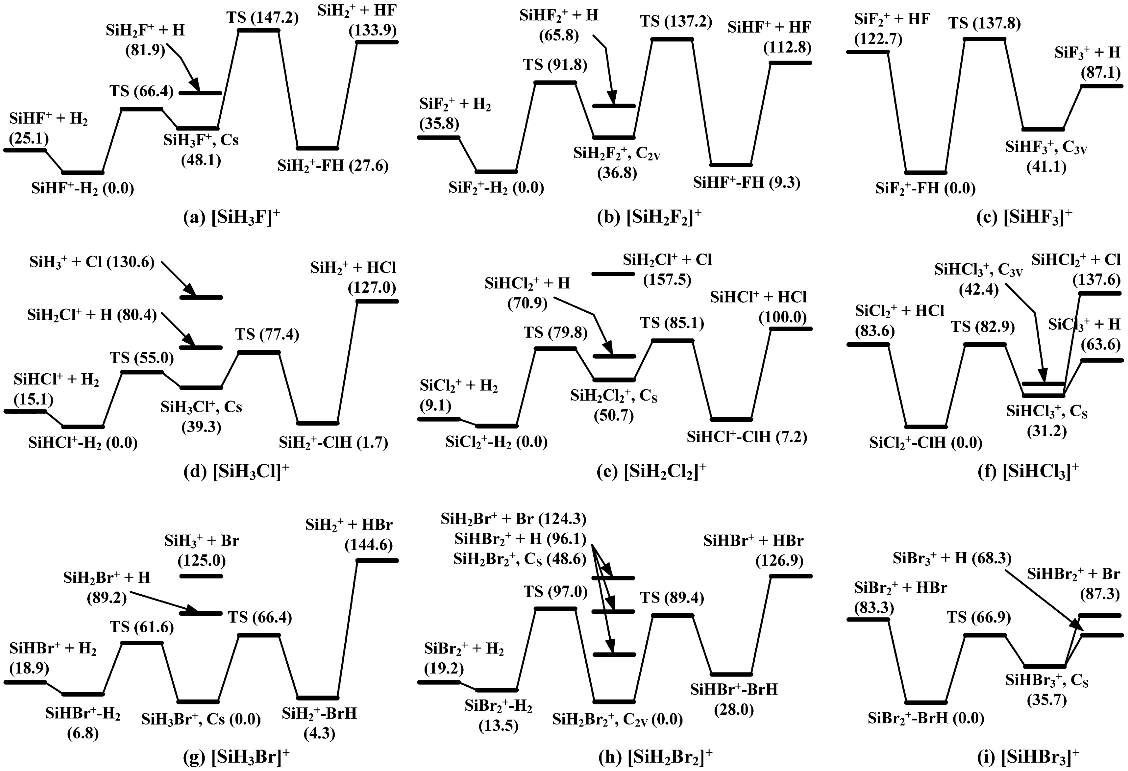

(a) $[SiH_3F]^+$ (b) $[SiH_2F_2]^+$ (c) $[SiHF_3]^+$

(d) $[SiH_3Cl]^+$ (e) $[SiH_2Cl_2]^+$ (f) $[SiHCl_3]^+$

(g) $[SiH_3Br]^+$ (h) $[SiH_2Br_2]^+$ (i) $[SiHBr_3]^+$

Fig. 9. Potential energy surfaces of $[SiH_3X]^+$, $[SiH_2X_2]^+$, and $[SiHX_3]^+$ cations (X = F, Cl, Br; relative energies in parentheses are in kJ/mol).

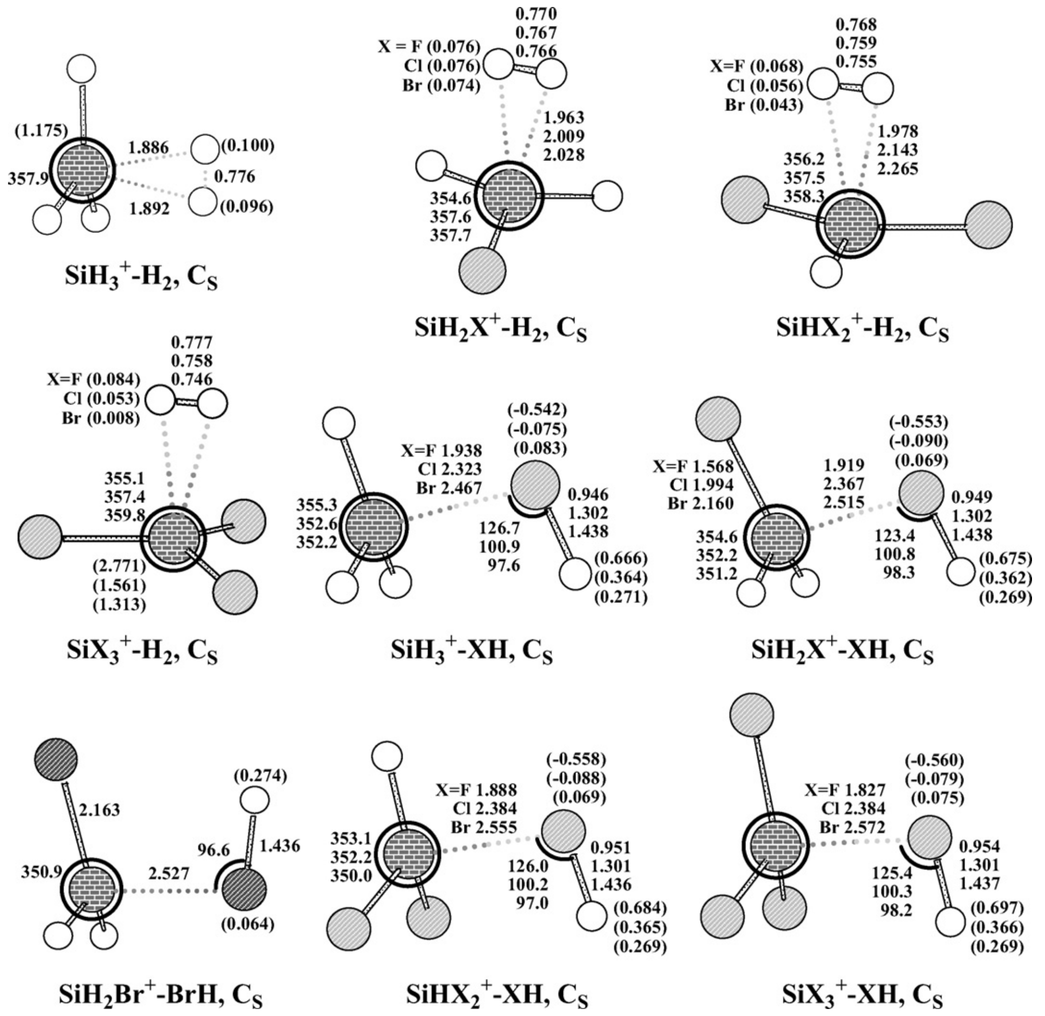

Fig. 10. Geometries of protonated silanes at B3LYP/6-31+G(2df,p) level (bond lengths in Å and angles in degree) and NBO charges (in parentheses, at CCSD(T)/6-31G(d) level), the values to the closed circles are the summations of three angles in silyl cations.

of 492.5 ± 5.0 kJ/mol (297 K) from proton transfer kinetics study to SiF_4 and of 496.6 kJ/mol from MP4 and QCISD(T) calculations with 6-311++G(3df,3pd) basis set, being higher than G3(CC) prediction of 473.5 kJ/mol.

3.6. Benchmark calculations for adiabatic IE_as of fluorinated species and PA of SiF_4

G3(CC) IE_a and PA of SiF_4 are significantly different from the previous experimental and theoretical studies. Benchmark calculations are carried out here for these two quantities at (U)CCSD(T,FC) level with cc-pV*n*Z basis sets (*n* = 3, 4, 5), while the core-valence correlation is considered with cc-pCVQZ basis set (only 1s orbitals of Si and F are frozen) [95]. The predicted IE_a are 15.38, 15.57, 15.62, and 15.59 eV, and PA_{298K} are 497.3, 485.9, 482.6, and 483.5 kJ/mol with basis sets cc-pV*n*Z (*n* = 3, 4, 5) and cc-pCVQZ, respectively. At CCSD(T)/VTZ level, the IE_a agrees with the ion-chemistry result of 15.29 ± 0.08 eV [42] and the CCSD(T)/AVTZ + MP2/CBS prediction of 15.34 eV [54], and PA agrees with the recent experimental proton-transfer and theoretical QCISD(T)/6-311++G(3df,3pd) studies of 492.5 ± 5.0 and 496.6 kJ/mol [92]. However, after basis set extrapolation and correction for core-valence correlation, the (U)CCSD(T) IE_a and PA of 15.67 eV and 478.9 kJ/mol support current G3(CC) results of 15.74 eV and 473.5 kJ/mol instead. Benchmark calculations also obtain adiabatic IE_as of 7.36, 10.75, 9.06, 9.49, 8.05, and 8.34 eV for SiF, SiF_2, SiF_3, SiHF, SiH_2F, and $SiHF_2$, respectively, comparing to G3(CC) values of 7.41, 10.91, 9.17, 9.47, 8.12, and 8.43 eV. The values for SiF and SiF_2 agree with previous RCCSD(T)/CBS values [54] of 7.36 and 10.74 eV, while values for SiF_3 is higher than RCCSD(T)/CBS of 8.98 eV, being in line with the case for $IE_a(SiF_4)$. The (U)CCSD(T)/CBS supports current G3(CC) calculations except for SiF_2, where G3(CC) IE_a is higher by *ca.* 0.16 eV. Surprisingly, the benchmark calculations support the previous BAC-MP4/6-31G(d,p) predictions of 7.21, 10.77, 9.09, 9.48, 8.05, and 8.33 eV [29], except for SiF and SiF_4, where the deviations were 0.15 and 0.40 eV, respectively.

3.7. Enthalpies of formation of halogenated silanes and cations (Tables 4 and 5)

The enthalpies of formation of silanes and the most stable silane cations are readily obtained from the G3(CC) atomization energies and the adiabatic IE_as. Evaluations by Walsh [27] and JANAF-1985 [26] have recommended $\Delta_f H^\circ_{298\,K} = -1615.0 \pm 0.8$, -662.7 ± 5.4, and -415.5 ± 8.4 kJ/mol for SiF_4, $SiCl_4$, and $SiBr_4$, compared to predictions of −1607.5, −655.0, and −415.8 kJ/mol using G3(CC) atomization energies (Table 4). The small discrepancies on SiF_4 and $SiCl_4$ are likely due to the deficiency of G3(CC) in describing the F–F or Cl–Cl interactions, therefore corrections of −1.25 and −1.3 kJ/mol are assigned to each F–F and Cl–Cl interaction, respec-

Table 3
ZPE, G3(CC)/B2df+ (in Hartree), the enthalpies of formation derived from atomization energies of protonated silanes, proton affinities at 0 K and 298 K, and $D_0(\text{Silyl}^+–H_2/HX)$ (in kJ/mol)

Germane	Germane-H$^+$	ZPE	G3(CC)	$\Delta_f H^\circ$		PA			D_0
				0 K	298 K	0 K	298 K [a]	Lit. (298 K) [b]	
SiH_4	$SiH_3{}^+–H_2$	0.03835	−291.99019	935.0	924.2	632.1	634.0	631.5 639.7 [c] 628–653 [d]	50.2
SiH_3F	$SiH_2F^+–H_2$	0.03405	−391.25602	572.3	561.4	**609.8**	**613.2**		**36.8**
	$SiH_3{}^+–FH$	0.03608	−391.24864	596.9	586.6	585.2	586.8	585.3	117.4
SiH_2F_2	$SiHF_2{}^+–H_2$	0.02903	−490.52647	195.5	186.5	**571.5**	**572.7**		**38.8**
	$SiH_2F^+–FH$ FSiFH—*cis*	0.03138	−490.52165	214.2	205.0	552.7	554.2	552.1	123.9
$SiHF_3$	$SiF_3{}^+–H_2$	0.02455	−589.79206	−167.1	−174.6	507.5	508.7		64.8
	$SiHF_2{}^+–FH$ HSiFH—*trans*	0.02632	−589.79725	−176.2	−183.6	**516.5**	**517.7**	515.4	**139.5**
SiF_4	$SiF_3{}^+–FH$ FSiFH—*cis*	0.02143	−689.06519	−546.0	−552.2	472.1	473.5	470.7 502.9 [c] 492.5 ± 5.0 [e] 478.9 [f]	172.8
SiH_3Cl	$SiH_2Cl^+–H_2$	0.03261	−751.50119	772.8	762.5	628.8	630.7		23.6
	$SiH_3{}^+–ClH$ HSiClH—*trans*	0.03362	−751.50466	766.3	756.0	**635.3**	**637.3**	634.3	**130.4**
SiH_2Cl_2	$SiHCl_2{}^+–H_2$	0.02570	−1211.01477	600.7	593.7	**625.6**	**625.9**		**12.6**
	$SiH_2Cl^+–ClH$ ClSiClH—*trans*	0.02757	−1211.01535	604.0	595.8	622.3	623.8	622.9	103.7
$SiHCl_3$	$SiCl_3{}^+–H_2$	0.01924	−1670.52721	432.8	428.5	**615.6**	**615.7**		**10.0**
	$SiHCl_2{}^+–ClH$ HSiClH—*trans*	0.02132	−1670.52905	433.3	427.5	**615.0**	**616.7**	614.9	**91.3**
$SiCl_4$	$SiCl_3{}^+–ClH$ ClSiClH—*trans*	0.01480	−2130.04143	265.5	262.3	609.6	611.5	609.1	88.8
SiH_3Br	$SiH_2Br^+–H_2$	0.03198	−2865.00406	831.9	831.9	634.7	636.5		19.5
	$SiH_3{}^+$-BrH HSiBrH—*trans*	0.03252	−2865.01019	817.2	817.2	**649.3**	**651.2**		**142.9**
SiH_2Br_2	$SiHBr_2{}^+–H_2$	0.02403	−5438.02076	717.2	717.2	641.6	641.1		7.9
	SiH_2Br^+-BrH BrSiBrH—*trans*	0.02652	−5438.02287	718.1	718.1	640.7	643.2		107.3
	SiH_2Br^+-BrH BrSiBrH—*cis*	0.02629	−5438.02234	718.9	718.9	639.9	641.9		108.1
$SiHBr_3$	$SiBr_3{}^+–H_2$	0.01583	−8011.03761	601.4	601.4	**647.6**	**644.4**		**6.6**
	$SiHBr_2{}^+$-BrH HSiBrH—*trans*	0.01970	−8011.03795	610.5	610.5	638.5	641.0		89.3
$SiBr_4$	$SiBr_3{}^+$-BrH BrSiBrH—*trans*	0.01214	−10584.05290	501.4	501.4	640.6	642.7		81.4

[a] Thermal correction of RT/2 is assigned to one of the low-frequency modes; Values in bold corresponds to the lowest protonated silanes; [b] From G3 prediction by Chien et al. [55], unless otherwise stated; [c] From Hunter and Lias [94]; [d] From Tandem mass spectrometry study by Cheng and Lampe [91]; [e] Mass spectrometry study [92]; [f] CCSD(T)/CBS with core-valence correlation by present study (see text).

tively. The corrections are applied to all other species with F–F or Cl–Cl interactions.

For $\Delta_f H^\circ_{298\,K}$ (SiH_4), Gunn and Green (GG) first obtained a value of 30.5 ± 1.3 kJ/mol from the heat of decomposition for $SiH_4(g) \rightarrow Si(s) + 2H_2(g)$ and values of 71.5 ± 1.3 and 108.4 kJ/mol for Si_2H_6 and Si_3H_8 [96,97]. These values are supported excellently by our G3(CC) predictions of 29.4, 70.0, and 106.9 kJ/mol, respectively. These calorimetric measurements have high precision. However, CATCH and JANAF argued that Si(*s*) produced was in amorphous state of in crystalline state, and raised the values by 4.2 kJ/mol per silicon atom, leading to fairly large discrepancies to G3(CC) predictions. The corrected values for SiH_4 and Si_2H_6 were adopted in photoionization study on SiH_x [31] and in a large number of theoretical studies on the thermochemistry of silicon hydrides [98–102] where they were taken as reference for calibrating the theory and setting up the correction parameters. However, Feller and Dixon [59] criticized this correction by CATCH and JANAF from their high-level CCSD(T)/CBS calculation of $\Delta_f H^\circ_{0\,K}(SiH_4) = 36.4 \pm 2.5$ kJ/mol and $\Delta_f H^\circ_{0\,K}(Si_2H_6) = 82.4 \pm 2.1$ kJ/mol ($\Delta_f H^\circ_{298\,K} = 26.8$ and 64.4 kJ/mol using current B3LYP thermal corrections), which supports the original GG values. Together with our G3(CC) predictions, the original GG value for SiH_4 is preferred.

Experimentally, $\Delta_f H^\circ$ of other halosilanes have been measured from the equilibrium studies, and the most notable were the systematic hydrogenation studies by Farber and Srivastava [103–105]. The measured enthalpies of reactions are compared with G3(CC) predictions as:

$$SiF_4 + H_2 \rightarrow SiHF_3 + HF,$$

$$\Delta_r H^\circ_{298\,K} = 116.3 \pm 8.4\ \text{kJ/mol (Expt)},\ 141.6\ \text{kJ/mol (G3(CC))}$$

$$SiHF_3 + H_2 \rightarrow SiH_2F_2 + HF$$

$$\Delta_r H^\circ_{298\,K} = 149.4 \pm 8.4\ \text{kJ/mol (Expt)},\ 154.0\ \text{kJ/mol(G3(CC))}$$

$$SiH_2F_2 + H_2 \rightarrow SiH_3F + HF$$

$$\Delta_r H^\circ_{298\,K} = 115.5 \pm 8.4\ \text{kJ/mol (Expt)},\ 143.1\ \text{kJ/mol(G3(CC))}$$

$$SiCl_4 + H_2 \rightarrow SiHCl_3 + HCl$$

$$\Delta_r H^\circ_{298\,K} = 71.1 \pm 6.3\ \text{kJ/mol (Expt)},\ 81.4\ \text{kJ/mol(G3(CC))}$$

$$SiHCl_3 + H_2 \rightarrow SiH_2Cl_2 + HCl$$

$$\Delta_r H^\circ_{298\,K} = 91.6 \pm 5.0\ \text{kJ/mol (Expt)},\ 86.4\ \text{kJ/mol(G3(CC))}$$

$$SiH_2Cl_2 + H_2 \rightarrow SiH_3Cl + HCl$$

$$\Delta_r H^\circ_{298\,K} = 87.0 \pm 6.3\ \text{kJ/mol (Expt)},\ 84.6\ \text{kJ/mol(G3(CC))}$$

$$SiBr_4 + H_2 \rightarrow SiHBr_3 + HBr$$

$$\Delta_r H^\circ_{298\,K} = 75.9 \pm 2.9\ \text{kJ/mol (Expt)},\ 77.4\ \text{kJ/mol(G3(CC))}$$

Table 4

ZPE, G3(CC)/B2df+ (in Hartree), the enthalpies of formation derived from atomization energies, along with other experimental and theoretical values (in kJ/mol)

Species[a]	ZPE	G3(CC)	0 K	298 K	298 K[b]	JANAF[c]	Walsh[d]	Previous (theoretical)	Experimental
Si	0.00000	−289.22263	446.0	450.0		446.0 ± 8			
Br	0.00000	−2573.51914	117.9	111.9		117.9			
HBr	0.00592	−2574.16348	−27.0	−34.9		−36.4			
SiH_4	0.03065	−291.74111	39.0	29.4		34.3 ± 2.1		35.3[e]	30.5 ± 1.3[l]
Si_2H_6	0.04797	−582.29870	88.0	70.0					71.5 ± 1.3[l]
Si_3H_8	0.0651	−872.85951	128.2	106.9					108.4[l]
SiH_3F	0.02678	−391.01578	−346.0	−355.3		−376.6 ± 20.9	−376.6 ± 41.8	−350.9[e], −357.7[f], −352.7[g], −359.0[h]	−415.9[m]
SiH_2F_2	0.02235	−490.30137	−761.2	−769.6	−770.9	−790.8 ± 20.9	−790.8 ± 33.6	−766.6[e], −779.8[f], −771.9[g] −779.5[h]	−804.2
$SiHF_3$	0.01743	−589.59083	−1187.8	−1194.7	−1198.5	−1200.8 ± 20.9	−1200.8 ± 20.9	−1193.1[e], −1207.6[f], −1201.2[g], −1205.8[h]	−1225.9
SiF_4	0.01224	−688.87534	−1602.1	−1607.5	−1615.0	−1615.0 ± 0.8	−1615.0 ± 0.8	−1607.1[e]	
SiH_3Cl	0.02575	−751.25413	−126.5	−135.6		−141.8 ± 8	−135.6 ± 10.5	−132.3[e], −134.7[f], −133.9[g]	
SiH_2Cl_2	0.02007	−1210.77007	−301.8	−309.2	−310.5	−320.5 ± 12.6	−315.1 ± 8.4	−308.7[e], −311.7[f], −310.5[i]	
$SiHCl_3$	0.01377	−1670.28638	−479.7	−484.6	−488.5	−496.2 ± 4.2	−499.2 ± 7.0	−487.2[e], −489.5[f], −488.7[i]	
$SiCl_4$	0.00703	−2129.80051	−653.0	−655.0	−662.8	−662.8 ± 1.3	−662.7 ± 5.4	−660.9[e], −662.8[f]	
SiH_3Br	0.02528	−2864.75492	−61.6	−77.9		−78.2 ± 17	−64.0 ± 8.8		
SiH_2Br	0.01909	−5437.77061	−169.3	−191.1		−190.4 ± 17	−180.7 ± 10.5		
$SiHBr_3$	0.01224	−8010.78642	−279.1	−305.2		−302.9 ± 17	−303.3 ± 9.2		
$SiBr_4$	0.00499	−10583.80076	−386.1	−415.8		−415.5 ± 16.7	−415.5 ± 8.4		
SiH_3	0.02081	−291.08650	200.7	195.2				200.0[f], 199.6[h],	195.0 ± 6.7[p]
SiH_2F	0.01704	−390.35694	−173.0	−178.3				−176.4[f], −187.9[h],	
$SiHF_2$	0.01260	−489.63831	−577.1	−581.5	−582.8			−584.0[f], −596.6[h],	
SiF_3	0.00807	−588.92119	−985.4	−988.3	−992.1	−1085.3 ± 16.7	−1000.0 ± 21.0	−993.4[f], −1007.1[h], −998.7[j],	−1075 ± 11[n] −997.5 ± 4.6[q]
SiH_2Cl	0.01616	−750.59932	36.3	31.2				32.6[f], 33.5[i],	
$SiHCl_2$	0.01072	−1210.11513	−138.1	−141.5	−142.8			−143.5[f], −142.3[i],	
$SiCl_3$	0.00477	−1669.63052	−312.6	−313.4	−317.3	−390.4 ± 16.7	−334.7 ± 8.4	−320.1[f], −317.1[i], −315.5[k]	
SiH_2Br	0.01575	−2864.10143	97.9	85.5					
$SiHBr_2$	0.00987	−5437.11884	−13.5	−31.4					
$SiBr_3$	0.00348	−8010.13641	−126.7	−148.8		−201.7 ± 63	−159.0 ± 25.2		
SiH_2-T	0.01178	−290.43496	356.4	354.8					
SiH_2-S	0.01146	−290.46571	274.8	273.1				284.9[f], 274.9[h],	270.3 ± 2.9
SiHF-T	0.00800	−389.69375	13.3	11.9					
SiHF-S	0.00816	−389.75282	−141.4	−143.0				−149.4[f], −158.2[h],	
SiF_2-T	0.00436	−488.94597	−312.2	−312.7					
SiF_2-S	0.00442	−489.06669	−629.0	−629.7	−631.0	−587.9 ± 12.6	−589.9 ± 8.4	−627.0[f], −640.2[h], −632.2[j]	−595.8 ± 6.7[n] −637.6 ± 6.3[q]
SiHCl-T	0.00734	−749.94238	206.7	205.5					
SiHCl-S	0.00746	−749.99584	66.7	65.3				71.1[f], 62.8[i],	
$SiCl_2$-T	0.00268	−1209.44624	65.8	66.1					
$SiCl_2$-S	0.00266	−1209.53194	−159.3	−159.0	−160.3	−168.6 ± 3.3	−168.6 ± 3.3	−157.3[f], −161.5[i], −165.1[k]	−159.0 ± 8.4[r]
SiHBr-T	0.00702	−2863.44651	263.3	254.7					
SiHBr-S	0.00716	−2863.49836	127.5	118.8					
$SiBr_2$-T	0.00199	−5436.45669	173.1	158.9					
$SiBr_2$-S	0.00201	−5436.53479	−32.0	−46.3		−52.3 ± 16.7	−46.0 ± 8.4		−46.0 ± 8.4
Si–H	0.00452	−289.84243	361.8	363.0	363.9	376.7 ± 8.4		383.7[f], 376.1[h],	369.0 ± 5.0[r]
Si–F	0.00181	−389.13407	−64.7	−63.5	−62.6	−20.1 ± 12.6	−20.9 ± 25.2	−52.0[f], −59.4[h], −58.6[j]	
Si–Cl	0.00114	−749.37761	142.0	143.5	144.6	198.3 ± 6.7	154.8 ± 41.8	158.6[f], 152.7[i], 152.7[k]	154.8 ± 8.4[r]
Si–Br	0.00090	−2862.88131	199.9	193.9	194.9	235.3 ± 46.0	196.6 ± 41.8		203.8 ± 8.4[r]

[a] T—triplet state, S—singlet state; [b] With corrections of −1.25 and −1.3 kJ/mol per F–F and Cl–Cl interactions, respectively (see text for detail); for Si–X, the thermal correction from Π-doublet of ground state are included; [c] JANAF-1985 [26]; [d] Evaluation by Walsh [27]; [e] From G3 atomization energies [55]; [f] BAC-MP4 calculation, using 34.3 ± 2.1 kJ/mol for the enthalpy of formation of SiH_4, for silicon hydrides and chlorinated compounds [48], and fluorinated compounds [47]; [g] Fluorinated silanes at MP4/6-31G(d,p) level using isodesmic reactions [49]; [h] MP4/6-31++G(2d,2p) with isodesmic reactions based on experimental SiH_n and SiF_4 [17]; [i] Chlorinated compounds at MP4/6-31+G(2df,p) level using isodesmic reactions [50]; [j] SiF_x (x = 1–3), from the calculated CCSD(T)/CBS bond dissociation energies [54]; [k] $SiCl_x$ (x = 1–3), from the calculated G2(MP2) bond dissociation energies [51]; [l] From heat of decomposition [96,97]; [m] Chemical equilibrium; [n] From threshold energies in reaction of $Si^+ + SiF_4$ [40]; [p] From photoionization of SiH_x [31]; [q] From collision-induced dissociation and charge transfer reactions [41]; [r] From chemical equilibrium study [28].

$$SiHBr_3 + H_2 \rightarrow SiH_2Br_2 + HBr$$

$$\Delta_r H^\circ_{298\,K} = 86.2 \pm 6.3\ \text{kJ/mol (Expt)},\ 80.8\ \text{kJ/mol(G3(CC))}$$

$$SiH_2Br_2 + H_2 \rightarrow SiH_3Br + HBr$$

$$\Delta_r H^\circ_{298\,K} = 80.3 \pm 2.1\ \text{kJ/mol (Expt)},\ 79.9\ \text{kJ/mol(G3(CC))}$$

where halosilanes were quantified using electron impact ionization mass spectrometry. Large discrepancies between measurements and G3(CC) are observed for hydrogenation of SiF_4, SiH_2F_2, and $SiCl_4$. Possible source of error in the experiment is the concentration determination, where the observed appearance energies for SiH_3F, SiH_2F_2, $SiHF_3$, and $SiHCl_3$ are 13.0, 11.0, 11.0 ± 1.0 eV, and 12.5 ± 1 eV, being significantly different from the G3(CC) vertical IEs of 12.93, 13.06, 14.60, and 12.00 eV and adiabatic IE_as of 11.81, 12.27, and 13.03, and 11.6 eV to structures closest to their neutrals (Table 1).

For $\Delta_f H^\circ_{298\,K}$ of fluorosilanes, both Walsh [27] and JANAF-1985 [26] preferred the estimations from linear interpolation between

SiH_4 and SiF_4 and disregarded the equilibrium studies by Farber and Srivastava [103]. Walsh claimed that "there is some unassessed source of error" in the experimental data but also agreed that fluorosilanes are most likely to deviate from linear interpolation. G3(CC) agrees with the linear interpolation estimations for $SiHF_3$ only, −1198.5 *vs* −1200.8 kJ/mol, and the discrepancies for SiH_3F and SiH_2F_2 are more than 20 kJ/mol. On the other hand, G3(CC) agrees with previous G3, BAC-MP4, and other MP4 prediction using isodesmic reactions [17,48,49,55].

For $\Delta_f H^\circ_{298\,K}$ of chlorinated and brominated silanes, Walsh [27] recommended the results from Farber and Srivastava [103–105]. Alternatively, JANAF-1985 [26] recommended $\Delta_f H^\circ_{298\,K}(SiHCl_3) = -496.2 \pm 4.2$ kJ/mol from the averaged enthalpy difference between $SiHCl_3$ and $SiCl_4$ from the equilibrium studies, and applied linear interpolation to SiH_2Cl_2 and SiH_3Cl. For bromosilanes, JANAF-1985 [26] suggested values of -78.2 ± 17, -190.4 ± 17, and -302.9 ± 17 kJ/mol for SiH_3Br, SiH_2Br_2, and $SiHBr_3$ from the linear interpolation between SiH_4 and $SiBr_4$ (using the original GG value for SiH_4). Values for SiH_3Cl, SiH_2Cl_2, and $SiHCl_3$ from Walsh (-135.6 ± 10.5, -315.1 ± 8.4, and -499.2 ± 7.0 kJ/mol) and JANAF-1985 (-141.8 ± 8, -320.5 ± 12.6, and -496.2 ± 4.2 kJ/mol) agree closely within 6 kJ/mol, while those by Walsh agree slightly better with our G3(CC) predictions (−135.6, −310.5, and −488.5 kJ/mol). The JANAF values for bromosilanes are in excellent agreement with our G3(CC) predictions within 2 kJ/mol, while Walsh's recommendations are differed to G3(CC) values by 10 kJ/mol or more for SiH_2Br_2 and SiH_3Br. The G3(CC) results also agree closely with previous G3, BAC-MP4, and MP4 calculations on chlorosilanes with isodesmic reaction schemes [47,49,55].

Enthalpies of formation of the most stable silane cations are also predicted here using the G3(CC) results for neutral and the adiabatic IE_as (Table 5). For ion complex structures, one of the low-frequency vibrational modes is treated as internal rotation. The experimental studies were available to $SiH_4{}^+$ and $SiF_4{}^+$ only. Alternatively, theoretical studies were available to $SiF_x{}^+$ at CCSD(T)/CBS level [54], $SiH_xF_{4-x}{}^+$ at MP4/6-31G(d,p) level [29], and $SiCl_x{}^+$ at G2MP2 level [51].

For $SiH_4{}^+$, Berkowitz et al. [31] obtained $\Delta_f H^\circ_{0\,K} = 1101.2 \pm 3.4$ kJ/mol from the adiabatic IE(SiH_4) (with original GG value for SiH_4), with which the G3(CC) value of 1104.7 kJ/mol agrees excellently. For $SiF_4{}^+$, the results $\Delta_f H^\circ_{0\,K} = -132.6 \pm 5.6$ kJ/mol and $\Delta_f H^\circ_{298\,K} = -135.9 \pm 5.6$ kJ/mol from Fisher et al. [41] are lower than G3(CC) values of −91.2 and −95.3 kJ/mol because of the discrepancy in the calculated and measured IE_a as discussed in previous section. Theoretically, Bauschlicher et al. [51] predicted $\Delta_f H^\circ_{0\,K}(SiCl_4{}^+ - C_{2V}) = 465.7$ and $\Delta_f H^\circ_{298\,K} = 464.5$ kJ/mol for $SiCl_4{}^+$-C_{2V} from G2MP2 calculations for cation with C_S symmetry, being slightly higher than our G3(CC) values of 453.6 and 452.3 kJ/mol for $SiCl_4{}^+$-C_{2V}. Ignacio and Schlegel [29] also predicted values of 735.6, 350.7, −20.4, and −137.2 kJ/mol for $\Delta_f H^\circ_{298\,K}$ of SiH_3F^+, $SiH_2F_2{}^+$, $SiHF_3{}^+$, and $SiF_4{}^+$ based on MP4/6-31G(d,p) calculations with isodesmic reaction scheme. The differences to G3(CC) values of 738.6, 378.1, 18.7, and −95.3 kJ/mol increase with the degree of fluorination.

3.8. Enthalpies of formation of halogenated silyl, silylene, and silylidyne radicals and cations (Tables 4 and 5)

Walsh [27] and JANAF-1985 [26] have summarized early studies on SiX_n (X = H, F, Cl, Br) radicals. Recently, Hilderbrand et al. [28] obtained new values for $SiX_{1,2}$ (X = Cl, Br) from equilibrium studies. For cations, the experimental enthalpies of formation are available to $SiH_x{}^+$ [31,38,39], $SiF_x{}^+$ [40–42], $SiCl_x{}^+$ [43,44], and SiH_2Cl^+ and $SiHCl_2{}^+$ [45,46] from photoionization and ion-chemistry studies, from which the enthalpies for some of their neutral radicals were also derived. The results for $SiF_x{}^+$ and $SiCl_x{}^+$ carry large uncertainties as discussed above. Theoretical studies were also performed on $SiH_mF_n{}^{0,+1}$ at MP4/6-31G(d,p) level [29], on $SiF_n{}^{0,+1}$ at G2 and CCSD(T)/CBS level [54], and $SiCl_n{}^{0,+1}$ at G2(MP2) and CCSD(T)/AVQZ level [51].

3.8.1. SiH_x and $SiH_x{}^+$

Jasinski et al. [106] reviewed the experimental and theoretical studies on the thermochemistry of SiH_x radicals prior to 1995. Of the values listed, the ones from photoionization studies of SiH_x by Berkowitz et al. [31] were preferred. With the original GG value for SiH_4, $\Delta_f H^\circ_{0\,K}$ for SiH_3, SiH_2, and SiH are revised to 195.0 ± 6.7, 270.3 ± 2.9, and 369.0 ± 5.0 kJ/mol, respectively, being supported by G3(CC) predictions of 200.7, 274.8, and 361.8 kJ/mol, and previous CCSD(T)/CBS studies [59].

There have been several studies on the enthalpy of formation of SiH^+. JANAF-1985 [26] adopted the value by Douglas and Lutz [107], who derived $\Delta_f H^\circ_{0\,K} = 1140.3 \pm 11.3$ kJ/mol from the estimated $D_0(Si^+{-}H)$ using w_e and $w_e x_e$ of the excited A-state of SiH^+. Later, Elkind and Armentrout [39] reported $\Delta_f H^\circ_{0\,K} = 1135.6 \pm 5.9$ kJ/mol, from $D_0(Si^+{-}H) = 3.23 \pm 0.04$ eV obtained from threshold behavior of $Si^+ + H_2 \rightarrow SiH^+ + H$. Berkowitz et al. [31] reported more decisive $\Delta_f H^\circ_{0\,K} = 1133.8 \pm 5.0$ kJ/mol from photoionization study (corrected to GG's original value for SiH_4). G3(CC) predicts $\Delta_f H^\circ_{0\,K} = 1127.8$ kJ/mol ($\Delta_f H^\circ_{298\,K} = 1129.1$ kJ/mol), which supports the value by Berkowitz et al.

For $SiH_2{}^+$, Berkowitz et al. obtained $\Delta_f H^\circ_{0\,K} = 1153 \pm 2.5$ kJ/mol from appearance energy of $SiH_2{}^+ + H_2$ from photoionization of SiH_4 [31], and Boo and Armentrout obtained a closely agreed value of 1151 ± 7 kJ/mol from the endothermicity of reactions $Si^+ + C_2H_6/C_3H_8/C_2H_4/C_2D_6 \rightarrow SiH_2{}^+/SiD_2{}^+ + C_2H_4/C_3H_6/C_2H_2/C_2D_4$ [38]. Our G3(CC) value of 1151.7 kJ/mol agrees with both values within their uncertainty ranges. For $SiH_3{}^+$, Berkowitz et al. also obtained $\Delta_f H^\circ_{0\,K} < 989.9$ kJ/mol from the appearance energy of $SiH_3{}^+$ [31], and Boo and Armentrout [38] obtained $\Delta_f H^\circ_{0\,K} = 987.4 \pm 8.4$ kJ/mol from $\Delta_r H^\circ_{0\,K}$ of 88.0 ± 4.8 kJ/mol for $Si^+ + SiH_4 \rightarrow SiH_3{}^+ + SiH$, comparing to G3(CC) of 80.0 kJ/mol. Both values agree excellently with our G3(CC) prediction of 987.1 kJ/mol. However, the agreement with the latter is fortuitous to some extend because of the cancellation of the differences between experiment and theory: $\Delta(\Delta_r H^\circ_{0\,K}) \sim 8$ kJ/mol, $-\Delta[\Delta_f H^\circ_{0\,K}(SiH)] \sim -13$ kJ/mol (374.9 ± 7.1 kJ/mol *vs* 361.8 kJ/mol), $\Delta[\Delta_f H^\circ_{0\,K}(Si^+)] \sim 2$ kJ/mol, and $\Delta[\Delta_f H^\circ_{0\,K}(SiH_4)] \sim 4$ kJ/mol (CATCH/JANAF revision).

3.8.2. SiX (X = F, Cl, Br) radicals

Enthalpies of formation of SiF, SiCl, and SiBr have been obtained from the equilibrium studies. Both JANAF-1985 [26] and Walsh [27] suggested $\Delta_f H^\circ_{298\,K}(SiF) \sim -20$ kJ/mol from equilibrium of $Si(g) + SiF_2 \rightarrow 2SiF$ using a dubious value for $\Delta_f H^\circ_{298\,K}(SiF_2)$. The value is significantly higher than our G3(CC) prediction of −62.6 kJ/mol and other theoretical values from −52 to −60 kJ/mol [29,54]. For $\Delta_f H^\circ_{298\,K}$ of SiCl and SiBr, Walsh [27] recommended 155 ± 42 and 197 ± 42 kJ/mol and JANAF [26] suggested higher values of 198.3 ± 6.7 and 235 ± 46 kJ/mol from equilibrium of $Si(g/s) + SiX_2 \rightarrow 2SiX$. Recently, Hilderbrand et al. [28] obtained $\Delta_f H^\circ_{298\,K}(SiCl) = 154.8 \pm 8.4$ kJ/mol and $\Delta_f H^\circ_{298\,K}(SiBr) = 203.8 \pm 8.4$ kJ/mol from the equilibria of $Si(g) + X \rightarrow SiX$. The values agreed with Walsh's recommendation, and are *ca.* 10 kJ/mol higher than our G3(CC) predictions of 144.6 and 194.9 kJ/mol, while the value for SiCl was supported by other theoretical predictions of 153–159 kJ/mol [47,50,51].

Table 5
The enthalpies of formation for the most stable cations derived from atomization energies, along with the literature values (in kJ/mol)

Neutral	Cations	$\Delta_f H^\circ$ [G3(CC)]		$\Delta_f H^\circ$ (literature values)	
		0 K	298 K	0 K	298 K
Si	Si^+	1229.9	1234.0	1232.2 ± 4^b	
SiH	SiH^+	1127.8	1129.1	1140.3 ± 11.3^c 1135.6 ± 5.9^e 1133.8 ± 5.0^f	1136.0^d
SiF	SiF^+	650.1	651.2		641.5^d, 706.8 ± 9.2^g 635.3 ± 4.6^h 651.1^j
SiCl	$SiCl^+$	850.1	851.3		909 ± 29^k 847 ± 10.5^l, 850.1^m
SiBr	$SiBr^+$	907.2	901.0		
SiH_2	$SiH_2{}^+$	1151.7	1150.1	1153 ± 2.5^f, 1151 ± 7^n	1140.6^d
SiHF	$SiHF^+$	772.0	770.5		753.6^d
SiF_2	$SiF_2{}^+$	422.7^a	422.0^a		449.9 ± 8.4^g, 404 ± 5^h 396.3^d, 403.8^j
SiHCl	$SiHCl^+$	950.8	949.4		
$SiCl_2$	$SiCl_2{}^+$	770.0^a	769.9^a		773.6 ± 10.9^l, 761.1^m
SiHBr	$SiHBr^+$	1000.7	991.9		
$SiBr_2$	$SiBr_2{}^+$	867.9	853.3		
SiH_3	$SiH_3{}^+$	987.1	981.5	$<989.9^f$, 987.4 ± 8.4^o	973.7^d
SiH_2F	SiH_2F^+	610.9	605.5		582.1^d
$SiHF_2$	$SiHF_2{}^+$	233.5^a	229.1^a		202.2^d
SiF_3	$SiF_3{}^+$	-104.2^a	-107.3^a		-105.5 ± 18.8^g -122.6 ± 2.5^p -137.6^d, -132.1^j
SiH_2Cl	SiH_2Cl^+	798.2	793.0		765.7 ± 16.8^q
$SiHCl_2$	$SiHCl_2{}^+$	613.8^a	610.1^a		585.0 ± 18.4^q
$SiCl_3$	$SiCl_3{}^+$	440.8^a	439.3^a		421 ± 13^k, 421.0^m
SiH_2Br	SiH_2Br^+	853.2	840.6		
$SiHBr_2$	$SiHBr_2{}^+$	726.9	708.7		
$SiBr_3$	$SiBr_3{}^+$	609.8	587.1		
SiH_4	$SiH_2{}^+–H_2$, C_S	1104.7	1096.9		1107.2^d
SiH_3F	$SiHF^+–H_2$, C_1	745.1	738.6		735.6^d
SiH_2F_2	$SiF_2{}^+–H_2$, C_S	385.1^a	378.1^{a*}		350.7^d
$SiHF_3$	$SiF_2{}^+–FH$, C_1	24.7^a	18.7^{a*}		-20.4^d
SiF_4	$SiF_4{}^+$, C_{2V}	-91.2^a	-95.3^a		-137.2^d, -133.8^j
SiH_3Cl	$SiHCl^+–H_2$, C_1	933.8	927.8		
SiH_2Cl_2	$SiCl_2{}^+–H_2$, C_S	759.0^a	755.5^{a*}		
$SiHCl_3$	$SiCl_2{}^+–ClH$, C_1	593.3^a	590.4^{a*}		
$SiCl_4$	$SiCl_4{}^+$, C_{2V}	453.6^a	452.3^a		445.7^m
SiH_3Br	SiH_3Br^+, C_S	980.0	965.0		
SiH_2Br_2	$SiH_2Br_2{}^+$, C_{2V}	846.8	825.5		
$SiHBr_3$	$SiBr_2{}^+–BrH$, C_1	757.5	732.8^*		
$SiBr_4$	$SiBr_4{}^+$, C_{2V}	629.4	600.0		

[a] Corrections for F–F and Cl–Cl interactions (−1.25 and −1.3 kJ/mol per interaction) applied; values with asterisk (*) have been corrected for thermal energy of internal rotation; [b] From JANAF table [26]; [c] From vibrational terms [107]; [d] From BAC-MP4/6-31G(d,p) [29]; [e] From reaction $Si^+ + H_2 \rightarrow SiH^+ + H$ [39]; [f] From photoionization, lowered by 1 kcal/mol [31]; [g] From ion chemistry [40]; [h] From ion chemistry [41]; [i] From BAC-MP4/6-31G(d,p) [29]; [j] From CCSD(T)/CBS [54]; [k] From ion chemistry [43]; [l] From ion chemistry [44]; [m] From CCSD(T)/AVQZ calculation [51]; [n] From ion-chemistry [38]; [o] From reaction $Si^+ + SiH_4 \rightarrow SiH_3{}^+ + SiH$ [38]; [p] From ion chemistry [42]; [q] From ion–molecule reaction [45,46].

3.8.3. *Silylene radicals*

For $\Delta_f H^\circ_{298\,K}(SiF_2)$, JANAF-1985 [26] and Walsh [27] suggested two closely agreed values of -587.9 ± 12.6 and -589.9 ± 8.4 kJ/mol. Afterwards, Fisher et al. [41] obtained a lower value of -637.6 ± 6.3 kJ/mol from the threshold energy for $Si^+ + SiF_4 \rightarrow SiF_2 + SiF_2{}^+$. Theoretical studies have obtained relatively consistent values in the range of −627 to −640 kJ/mol [29,54] and −631.0 kJ/mol from G3(CC), which support the later ion chemistry study. However, the agreement is fortuitous because the measured $\Delta_f H^\circ_{298\,K}$ $(SiF_2 + SiF_2{}^+)$ of -151.4 ± 12.6 kJ/mol from the threshold is much higher than the theoretical predictions of −243.9 kJ/mol from BAC-MP4/6-31G(d,p) [29], −228.4 kJ/mol from CCSD(T)/CBS [54], and −206.4 kJ/mol from G3(CC) here. Neither $\Delta_f H^\circ_{298\,K}(SiF_2)$ nor $\Delta_f H^\circ_{298\,K}(SiF_2{}^+)$ reported by Fisher et al. [41] was reliable.

For $SiCl_2$ and $SiBr_2$, JANAF-1985 [26] and Walsh [27] summarized the equilibrium studies on $Si(s/g) + SiCl_4/SiBr_4 \rightarrow 2SiCl_2/SiBr_2$ and obtained $\Delta_f H^\circ_{298\,K}(SiCl_2) = -168.6 \pm 3.3$ kJ/mol, and $\Delta_f H^\circ_{298\,K}(SiBr_2) = -52.3 \pm 16.7$ kJ/mol (JANAF) or -46.0 ± 8.4 kJ/mol (Walsh). Recently, Hilderbrand et al. [28] obtained $\Delta_f H^\circ_{298\,K} = -159.0 \pm 8.4$ and -46.0 ± 8.4 kJ/mol for $SiCl_2$ and $SiBr_2$ from equilibrium of $Si(g) + 2Cl/Br \rightarrow SiCl_2/SiBr_2$. The later values are supported excellently by G3(CC) predictions of −160.3 and −46.3 kJ/mol. The value for $SiCl_2$ is also supported by other theoretical predictions of −157 to −165 kJ/mol [47,50,51].

No experimental study is available for $\Delta_f H^\circ_{298\,K}$ (SiHX). G3(CC) predictions are −143.0, 65.3, and 118.8 kJ/mol for X = F, Cl, and Br, respectively. Previous theoretical studies have obtained $\Delta_f H^\circ_{298\,K}(SiHF) = -149.4$ kJ/mol at BAC-MP4 level [47] or −158.2 kJ/mol at MP4/6-31++G(2d,2p) level with isodesmic reaction [17], and $\Delta_f H^\circ_{298\,K}(SiHCl) = 71.1$ kJ/mol at BAC-MP4 level [48] or 62.8 kJ/mol at MP4/6-31+G(2df,p) level with isodesmic reaction [50]. Note that RHF wavefunction instability is found for ground states of SiHX, and UHF wavefunctions are used for post-HF calculations.

The singlet–triplet (S–T) separations of silylene radicals are important parameters in assessing the reactivity of their reactivity. The S–T experimental separations determined from spectroscopic data [66] are 87.8 ± 2.9 kJ/mol ($T_0 = 7340 \pm 240\,cm^{-1}$), 314.9 kJ/mol (26319 cm^{-1}), and 226.6 kJ/mol (18943 cm^{-1}) for SiH_2, SiF_2, and $SiCl_2$. Value of 78.2 kJ/mol (0.81 eV) for SiH_2 can also be inferred from the measured IEs for singlet (9.05 eV) and triplet (8.24 eV) [31]. The G3(CC) values of 316.8 and 225.1 kJ/mol for SiF_2 and $SiCl_2$ are in excellent agreement with the spectroscopic determination. The G3(CC) prediction of 81.6 kJ/mol for SiH_2 is slightly lower than the spectroscopic determination, while being in better agreement with the photoionization study. The increased S–T separations of 81.6 to 140.0 to 225.1 kJ/mol for SiH_2, SiHCl, and $SiCl_2$ at G3(CC) level are in accordance with the decreased reactivity, e.g., the increased barrier heights from −2 to 64 to 164 kJ/mol for their insertion to H_2 at CCSD(T)/CBS level [108], and the increasing barrier height and the decreasing A-factor from insertions of SiHCl and $SiCl_2$ to H_2 from kinetics study [109].

3.8.4. *SiX_3 (X = F, Cl, Br) radicals*

Using $D(F_3Si{-}H)$ and $D(Cl_3Si{-}H)$ of 419 ± 5 and 382 ± 6 kJ/mol from the kinetic iodination technique and the estimated $D(Br_3Si{-}H)$ of 364 ± 21 kJ/mol, Walsh [27] obtained $\Delta_f H^\circ_{298K}$ (SiX_3) of -1000 ± 21, -335 ± 8, and -159 ± 25.2 kJ/mol for X = F, Cl, and Br, respectively, comparing to G3(CC) values of −992.1, −317.3, and −148.8 kJ/mol. At G3(CC) level, the corresponding $D(SiX_3{-}H)$ values are 424.4, 384.2, and 374.4 kJ/mol. While the G3(CC) predictions on SiF_3 and $SiBr_3$ agree with Walsh's estimations, the discrepancy on $\Delta_f H^\circ_{298\,K}(SiCl_3)$ can be ascribed mostly to the differences in $\Delta_f H^\circ_{298\,K}(SiCl_3H)$. JANAF [26] also listed a significantly different set of values, where those for SiF_3 and $SiCl_3$ were from the equilibrium study of $SiX_2(g) + SiX_4(g) \rightarrow 2SiX_3(g)$ and that for $SiBr_3$ from the averaged Si–Br bond dissociation energy in $SiBr_4$. The results (-1085.3 ± 16.7, -390.4 ± 16.7, and -201.7 ± 6.3 kJ/mol) are significantly lower than the G3(CC) predictions. For SiF_3, the G3(CC) result also agrees with previous predictions from −993 to −1007 kJ/mol for SiF_3 at levels of BAC-MP4 [48], MP4 with isodesmic reaction [17,29], and CCSD(T)/CBS [54] etc, and similarly for $SiCl_3$ at MP4 level with isodesmic reaction schemes [48,50] and G2MP2 level [51].

3.8.5. *SiF^+, $SiF_2{}^+$, and $SiF_3{}^+$*

Weber and Armentrout [40] first reported $\Delta_f H^\circ_{298\,K}$ of 706.8 ± 9.2, 449.9 ± 8.4, and -105.5 ± 18.8 kJ/mol ($\Delta_f H^\circ_{0\,K}$ of 705.7, 450.6, and −102.4 kJ/mol using present B3LYP thermal corrections) for SiF^+, $SiF_2{}^+$, and $SiF_3{}^+$, respectively, from the measured thresholds for reactions $Si^+ + BF_3 \rightarrow SiF^+ + BF_2$, $Si^+ + SiF_4 \rightarrow SiF_2 + SiF_2{}^+$, and $Si^+ + SiF_4 \rightarrow SiF_3{}^+ + SiF$, respectively. $\Delta_f H^\circ_{298\,K}(SiF^+)$ was unacceptable because $\Delta_f H^\circ_{298\,K}(BF_2)$ of -589.9 ± 4.2 kJ/mol used there is markedly lower than the recent CCSD(T)/CBS prediction of −497.5 kJ/mol [110]. Neither $\Delta_f H^\circ_{298\,K}(SiF_2{}^+)$ was reliable as discussed above. The measured threshold of 239.2 ± 13.5 kJ/mol for $SiF_3{}^+$ is also significantly higher than G3(CC) prediction of 207.0 kJ/mol, even though the resulted $\Delta_f H^\circ_{298\,K}(SiF_3{}^+)$ agrees with G3(CC) prediction of −107.3 kJ/mol.

The results for SiF^+ and $SiF_2{}^+$ by Weber and Armentrout [40] were later disregarded by Fisher et al. [41], who instead reported $\Delta_f H^\circ_{298\,K} = 635.2 \pm 4.6$ and 404 ± 5 kJ/mol for SiF^+ and $SiF_2{}^+$ from measured $D_0(Si^+{-}F) = 679.3 \pm 5.8$ kJ/mol, $D_0(SiF^+{-}F) = 306.8 \pm 3.9$ kJ/mol from the collision-induced dissociation studies. The measured $D_0(Si^+{-}F)$ is significantly higher than the theoretical predictions of 647.6 (G2 [54]), 663.1 (CCSD(T)/CBS [53,54]), and 657.1 (G3(CC)) kJ/mol, and the measured $D_0(SiF^+{-}F)$ is supported by G3(CC) prediction of 304.5 kJ/mol. Consequently, the results for SiF^+ and $SiF_2{}^+$ by Fisher et al. [41] are systematically lowered than G3(CC) values by 15–20 kJ/mol while being supported by BAC-MP4/6-31G(d,p) predictions of 641.5 and 396.3 kJ/mol [29]. $\Delta_f H^\circ_{298\,K}(SiF_3{}^+)$ was also re-determined by Kickel et al. [42] as −126.1 kJ/mol, being lower than G3(CC) values of −107.3 kJ/mol at 298 K, higher than BAC-MP4/6-31G(d,p) of −137.6 kJ/mol [29], and agreeing with CCSD(T)/CBS of −132.1 kJ/mol [54].

3.8.6. *$SiCl^+$, $SiCl_2{}^+$, and $SiCl_3{}^+$*

The earlier measurements on $SiCl^+$ using the appearance energies from $SiCl_2$ were rather diverse, e.g., two appearance energies were reported as 12.50 ± 0.10 eV [73] and 11.8 ± 0.2 eV [111]. Alternatively, Weber and Armentrout [43] obtained $\Delta_f H^\circ_{298\,K}(SiCl^+) = 902 \pm 29$ kJ/mol and $\Delta_f H^\circ_{298\,K}(SiCl_2{}^+) = 774 \pm 11$ kJ/mol from thresholds for reactions of $Si^+ + SiCl_4 \rightarrow SiCl^+ + Cl + SiCl_2$ and $Si^+ + SiCl_4 \rightarrow SiCl_2{}^+ + SiCl_2$. The measured threshold of 280 ± 29 kJ/mol for the first reaction is significantly higher than G3(CC) prediction of 240.1 kJ/mol, and the second threshold of 39 ± 10 kJ/mol coincidences with G3(CC) of 40.3 kJ/mol. The results were uncertain because $\Delta_f H^\circ_{298\,K}(SiCl_2)$ was not well established. Later, Fisher and Armentrout [44] disregarded the results and reported two new values of 847 ± 10.5 and 773.6 ± 10.9 kJ/mol for the enthalpies of formation of $SiCl^+$ and $SiCl_2{}^+$ from reaction thresholds of $Ar^+ + SiCl_4 \rightarrow Ar + SiCl^+ + Cl + Cl_2$ and $Ar^+ + SiCl_4 \rightarrow Ar + SiCl_2{}^+ + 2Cl$. The measured thresholds of 16.91 and 17.34 eV are supported by G3(CC) predictions of 16.89 and 17.24 eV, respectively. Consequently, the resulted enthalpies of formation are supported by G3(CC) predictions of 851.3 and 771.1 kJ/mol and CCSD(T)/AVQZ predictions [51] of 850.1 and 761.1 kJ/mol for $SiCl^+$ and $SiCl_2{}^+$, respectively.

For $SiCl_3{}^+$, Weber and Armentrout [43] first proposed $\Delta_f H^\circ_{298\,K} = 421 \pm 13$ kJ/mol from simple average of a few appearance energies of $SiCl_3{}^+$ from dissociative ionization of $SiCl_4$ and $HSiCl_3$. Fisher and Armentrout [44] later reported value of 411 ± 6.7 kJ/mol from threshold of $O_2{}^+ + SiCl_4 \rightarrow O_2 + SiCl_3{}^+ + Cl$, being lower than the theoretical predictions are 421.0 kJ/mol at CCSD(T)/CBS level [51] and 439.3 kJ/mol at G3(CC) level.

Compared to previous theoretical studies, G3(CC) values of 851.3, 769.8, 439.3, and 452.3 kJ/mol for $\Delta_f H^\circ_{298\,K}$ ($SiCl_n{}^+$, $n = 1$–4) agree with the G2(MP2) results of 857.0, 773.7, 439.8, and 464.5 kJ/mol for $SiCl^+$, $SiCl_2{}^+$, and $SiCl_3{}^+$, and with the CCSD(T)/AVQZ ones of 850.7, 754.9, 421.0, and 445.7 kJ/mol [51] on $SiCl^+$ and $SiCl_4{}^+$ only.

3.8.7. *SiH_2Cl^+ and $SiHCl_2{}^+$*

Murthy and Beauchamp [45,46] measured the energetics of SiH_2Cl^+ and $SiHCl_2{}^+$ relative to $SiCl_3{}^+$ from the kinetics of the following ion–molecular reactions:

$$SiCl_3{}^+ + SiHCl_3 \rightarrow SiHCl_2{}^+ + SiCl_4$$

$$\Delta_r H^\circ_{298\,K} = -0.4 \pm 0.8\,\text{kJ/mol(Expt)},\ -2.2\,\text{kJ/mol(G3(CC))}$$

$$SiCl_3{}^+ + SiH_2Cl_2 \rightarrow SiHCl_2{}^+ + SiHCl_3$$

$$\Delta_r H^\circ_{298\,K} = -3.8 \pm 1.3\,\text{kJ/mol(Expt)},\ -7.3\,\text{kJ/mol(G3(CC))}$$

$$SiCl_3{}^+ + SiH_2Cl_2 \rightarrow SiH_2Cl^+ + SiCl_4$$

$$\Delta_r H^\circ_{298\,K} = 2.9 \pm 1.3\,\text{kJ/mol(Expt.)},\ 4.0\,\text{kJ/mol(G3(CC))}$$

$$SiHCl_2{}^+ + SiH_2Cl_2 \rightarrow SiH_2Cl^+ + SiHCl_3$$

$$\Delta_r H^\circ_{298\,K} = 4.2 \pm 0.8\,kJ/mol(Expt),\ 6.3\,kJ/mol(G3(CC))$$

$$SiHCl_2{}^+ + SiH_3Cl \rightarrow SiH_2Cl^+ + SiH_2Cl_2$$

$$\Delta_r H^\circ_{298\,K} = 5.9 \pm 1.3\,kJ/mol(Expt),\ 8.0\,kJ/mol(G3(CC))$$

$$SiHCl_2{}^+ + SiH_4 \rightarrow SiH_2Cl^+ + SiH_3Cl$$

$$\Delta_r H^\circ_{298\,K} = 12.1 \pm 1.3\,kJ/mol(Expt),\ 16.7\,kJ/mol(G3(CC))$$

The G3(CC) enthalpies of reactions are in close agreement with the measurements, and the enthalpy differences between SiH_2Cl^+ and $SiHCl_2{}^+$ to $SiCl_3{}^+$, 349.8 and 168.1 kJ/mol, are in accordance with the experimental values of 354.4 ± 10.0 and 173.6 ± 11.7 kJ/mol, respectively. The resulted $\Delta_f H^\circ_{298\,K}(SiHCl_2{}^+) = 585.0 \pm 18.4$ kJ/mol and $\Delta_f H^\circ_{298\,K}(SiH_2Cl^+) = 765.7$ kJ/mol are lower than G3(CC) predictions of 610.1 and 793.0 kJ/mol. The discrepancies arise mainly from their adoption of $\Delta_f H^\circ_{298\,K}(SiCl_3{}^+) = 411 \pm 6.7$ kJ/mol from Fisher and Armentrout [44].

To our knowledge, no experimental study is available on the enthalpies of formation for other radical and cations. A value for $SiBr_3{}^+$ might be inferred from its appearance energy of 11.31 ± 0.03 eV in photoionization of $SiBr_4$ [75], which is lower than G3(CC) prediction of 11.54 eV. Theoretically, Ignacio and Schlegel [29] carried out MP4/6-31G(d,p) calculations on the enthalpies of formation of the fluorinated species and cations. Their results are systematically lower than our G3(CC) ones, and the discrepancies increase with the degree of fluorination to ~50 kJ/mol for $SiF_4{}^+$, −138.8 kJ/mol by BAC-MP4 and −87.8 kJ/mol by G3(CC).

4. Conclusions

We have carried out a systematic study on fluorinated, chlorinated, and brominated silanes, radicals, and cations, on their structures, ionization energies, proton affinities of silanes, and the enthalpies of formation, at G3(CC) level. The results are compared extensively with previous experimental and theoretical studies. The hydrogenated cations are characterized by the existence of ion complex structures. The most stable cations of silylene and silyl radicals have their classical divalent and trivalent structures; while the most stable silane cations have their non-classical ion complexes except for those of SiH_3Br and SiH_2Br_2. The presence of non-classical ground state cations for silanes implies difficulty in obtaining their adiabatic IE_as using photoelectron or photoionization studies. Previous photoelectron spectroscopy studies reported indeed the vertical IEs which are supported by current G3(CC) calculations. The transition barriers also imply complication in determining the endothermicity of certain silylene$^+$ + H_2/HX channels from the appearance energies of silylene$^+$ in the dissociative photoionization of halogenated silanes.

At G3(CC) level, the calculated adiabatic IE_as of SiH_x agree with the experimental values obtained from photoionization studies [31,39]; while calculations reveal significantly uncertainties on the results for $SiF_x{}^{0,+1}$ and $SiCl_x{}^{0,+1}$ from studies on charge-transfer and/or collision-induced dissociation reactions by the Armentrout group [40–44]. The most intriguing discrepancy is on SiF_4, where the G3(CC) IE_a of 15.74 eV is significantly higher than the values of 15.29 ± 0.08 eV from experiment [42] and 15.34 eV at CCSD(T)/AVTZ + MP2/CBS level [54]. G3(CC) PA(SiF_4) is also higher than experimental value by *ca.* 20 kJ/mol However, G3(CC) $IE_a(SiF_4)$ is supported by current (U)CCSD(T)/CBS benchmark calculations, and similar for PA(SiF_4). G3(CC) calculations on adiabatic IE_as of fluorinated species are also supported by (U)CCSD(T)/CBS except for SiF_2 where the deviation is *ca.* 0.16 eV. Agreements and large disagreements are also found between G3(CC) and previous calculations from MP4 to CCSD(T)/CBS levels, especially for fluorinated cations [29,51,53–55,60].

The enthalpies of formation of halogenated silanes, radicals, and cations are predicted using G3(CC) atomization energies and the adiabatic IE_as. The results agrees excellently with the photoionization mass spectrometry studies on SiH_x and $SiH_x{}^+$ [31] and with previous theoretical predictions at correlation levels from BAC-MP4 to CCSD(T)/CBS on neutral silanes and free radicals [29,51,53–55,60]. However, the G3(CC) results have considerable discrepancies with the previous experimental and theoretical values on the enthalpies of formation of cations, especially on fluorinated cations. We have assessed the experimental results on $SiF_x{}^{0,+1}$ and $SiCl_x{}^{0,+1}$ [40–44] and found that they carry considerable uncertainties. While our G3(CC) calculations on chlorinated and brominated species have normal “chemical accuracy” (~1 kcal/mol), the results on fluorinated species, especially on $SiF_2{}^+$, show large discrepancies to previous CCSD(T) and BAC-MP4/6-31G(d,p) and current (U)CCSD(T)/CBS calculations.

Supporting information

The B3LYP/6-31+G(2df,p) vibrational frequencies are listed in Tables S1–S3.

Acknowledgements

We thank for the service of high performance grid computing platform SCUTGrid provided by Information Network Research and Engineering Center of South China University of Technology and financial support from National Science Foundation of China (No. 20777017).

Appendix A. Supplementary data

Supplementary data associated with this article can be found, in the online version, at doi:10.1016/j.ijms.2008.07.004.

References

[1] C.K. Oh, S.D. Park, H.C. Lee, J.W. Bae, G.Y. Yeom, Electrochem. Solid-State Lett. 10 (2007) H94.
[2] Z. Wang, Y. Lou, J. Mater. Sci 42 (2007) 9920.
[3] M. Kogelschatz, G. Cunge, N. Sadeghi, J. Phys. D 37 (2004) 1954.
[4] G. Cunge, M. Kogelschatz, N. Sadeghi, J. Appl. Phys. 96 (2004) 4578.
[5] K.L. Williams, E.R. Fisher, J. Vac. Sci. Technol. A 21 (2003) 1024.
[6] A. Campo, C. Cardinaud, G. Turban, J. Vac. Sci. Technol. B 13 (1995) 235.
[7] S.K. Murad, S.P. Beaumont, M. Holland, C.D.W. Wilkonson, J. Vac. Sci. Technol. B 13 (1995) 2344.
[8] S. Yagi, N. Takahashi, Appl. Phys. Lett. 61 (1992) 2677.
[9] H.O. Pierson, Handbook of Chemical Vapor Deposition, Noyes Publications/William Andrew Publishing LLC, New York, 1999.
[10] K.L. Choy, Prog. Mater. Sci. 48 (2003) 57.
[11] T. Sakai, A. Sakai, H. Okano, Jpn. J. Appl. Phys. 32 (1993) 3089.
[12] C.C. Cheng, K.V. Guinn, V.M. Donnelly, J. Vac. Sci. Technol. B 14 (1996) 85.
[13] J. Tanaka, G. Miya, J. Vac. Sci. Technol. A 25 (2007) 353.
[14] J. Hanna, K. Shimizu, J. Organomet. Chem. 611 (2000) 531.
[15] T. Kudo, S. Nagase, Chem. Phys. 122 (1988) 233.
[16] M.N. Paddon-Row, S.S. Wong, Chem. Commun. (1987) 1585.
[17] E.W. Ignacio, H.B. Schlegel, J. Chem. Phys. 92 (1990) 5404.
[18] K.K. Das, K. Balasubramanian, J. Chem. Phys. 93 (1990) 5883.
[19] T. Kudo, S. Nagase, Chem. Phys. Lett. 148 (1988) 73.
[20] D. Balamurugan, M.K. Harbola, R. Prasad, Phys. Rev. A 69 (2004) 033201.
[21] P. Jackson, N. Sandig, M. Diefenbach, D. Schroder, H. Schwartz, R. Srinivas, Chem. Eur. J. 7 (2001) 151.
[22] P. Antoniotti, S. Borocci, N. Bronzolino, M. Giordani, F. Grandinetti, Eur. J. Inorg. Chem. (2006) 3010.
[23] L. Wang, J. Zhang, J. Phys. Chem. A 112 (2008) 3454.
[24] J. Berkowitz, G.B. Ellison, D. Gutman, J. Phys. Chem. 98 (1994) 2744.
[25] J.B. Pedley, B.S. Iseard, CATCH Table for Silicon Compounds, University of Sussex, 1972.

[26] M.W.J. Chase, C.A. Davies, J.R.H. Downey, D.J. Fruip, R.A. McDonald, A.N. Syverud, J. Phys. Chem. Ref. Data 14 (1985).
[27] R. Walsh, J. Chem. Soc. Faraday Trans. 1 79 (1983) 2233.
[28] D.L. Hildenbrand, K.H. Lau, A. Sanjurjo, J. Phys. Chem. A 107 (2003) 5448.
[29] E.W. Ignacio, H.B. Schlegel, J. Phys. Chem. 94 (1990) 7439.
[30] L. Wang, J. Zhang, J. Phys. Chem. 108 (2004) 10346.
[31] J. Berkowitz, J.P. Greene, H. Cho, B. Ruscis, J. Chem. Phys. 86 (1987) 1235.
[32] H. Bredohl, J. Breton, I. Dubois, J.M. Esteva, D. Macau-Hercot, F. Remy, J. Mol. Spectrosc. 199 (1999) 281.
[33] G. Bosser, H. Bredohl, I. Dubois, J. Mol. Spectrosc. 106 (1984) 72.
[34] H. Bredohl, J. Breton, I. Dubois, J.M. Esteva, D. Macau-Hercot, F. Remy, J. Mol. Spectrosc. 197 (1999) 28.
[35] A. Marijnissen, J.J. ter Meulen, Chem. Phys. Lett. 263 (1996) 803.
[36] R.D.J. Johnson, B.P. Tsai, J.W. Hudgens, J. Chem. Phys. 91 (1989) 3340.
[37] L.A. Kuznetsova, N.E. Kuz'menko, Y.Y. Kuzyakov, Opt. Specktros 24 (1968) 812.
[38] B.H. Boo, P.B. Armentrout, J. Am. Chem. Soc. 109 (1987) 3549.
[39] J.E. Elkind, P.B. Armentrout, J. Phys. Chem. 88 (1984) 5454.
[40] M.E. Weber, P.B. Armentrout, J. Chem. Phys. 88 (1988) 6898.
[41] E.R. Fisher, B.L. Kickel, P.B. Armentrout, J. Phys. Chem. 97 (1993) 10204.
[42] B.L. Kickel, E.R. Fisher, P.B. Armentrout, J. Phys. Chem. 97 (1993) 10198.
[43] M.E. Weber, P.B. Armentrout, J. Phys. Chem. 93 (1989) 1596.
[44] E.R. Fisher, P.B. Armentrout, J. Phys. Chem. 95 (1991) 4765.
[45] S. Murthy, J.L. Beauchamp, J. Phys. Chem. 96 (1992) 1247.
[46] S. Murthy, J.L. Beauchamp, J. Phys. Chem. 99 (1995) 9118.
[47] P. Ho, M.E. Coltrin, J.S. Binkley, C.F. Melius, J. Phys. Chem. 89 (1985) 4647.
[48] P. Ho, C.F. Melius, J. Phys. Chem. 94 (1990) 5120.
[49] E.W. Ignacio, H.B. Schlegel, J. Phys. Chem. 96 (1992) 5830.
[50] M.-D. Su, H.B. Schlegel, J. Phys. Chem. 97 (1993) 8732.
[51] C.W.J. Bauschlicher, H. Partridge, Chem. Phys. Lett. 276 (1997) 47.
[52] M.T. Swihart, R.W. Carr, J. Phys. Chem. A 101 (1997) 7434.
[53] A. Ricca, C.W.J. Bauschlicher, Chem. Phys. Lett. 287 (1998) 239.
[54] A. Ricca, C.W.J. Bauschlicher, J. Phys. Chem. A 102 (1998) 876.
[55] S.-H. Chien, W.-K. Li, N.L. Ma, J. Phys. Chem. A 104 (2000) 11398.
[56] L.A. Curtiss, K. Raghavachari, P.C. Redfern, G. Kedziora, J.A. Pople, J. Phys. Chem. A 105 (2001) 227.
[57] M.D. Allendrof, C.F. Melius, J. Phys. Chem. A 106 (2002) 6370.
[58] R. Janoschek, W.M.F. Fabian, J. Mol. Struct. 780/781 (2006) 80.
[59] D. Feller, D.A. Dixon, J. Phys. Chem. A 103 (1999) 6413.
[60] J. Hrusak, Z. Herman, S. Iwata, Int. J. Mass. Spectrom. 192 (1996) 165.
[61] E. Sicilia, M. Toscano, T. Mineva, N. Russo, Int. J. Quant. Chem. 61 (1997) 571.
[62] L.A. Curtiss, K. Raghavachari, P.C. Redfern, A.G. Baboul, J.A. Pople, Chem. Phys. Lett. 314 (1999) 101.
[63] L.A. Curtiss, K. Raghavachari, P.C. Redfern, V. Rassolov, J.A. Pople, J. Chem. Phys. 109 (1998) 7764.
[64] L.A. Curtiss, P.C. Redfern, K. Raghavachari, J.A. Pople, J. Chem. Phys. 114 (2001) 108.
[65] M.J. Frisch, G.W. Trucks, H.B. Schlegel, G.E. Scuseria, M.A. Robb, J.R. Cheeseman, J.A. Montgomery, T. Vreven, K.N. Kudin, J.C. Burant, J.M. Millam, S.S. Iyengar, J. Tomasi, V. Barone, B. Mennucci, M. Cossi, G. Scalmani, N. Rega, G.A. Petersson, H. Nakatsuji, M. Hada, M. Ehara, K. Toyota, R. Fukuda, J. Hasegawa, M. Ishida, T. Nakajima, Y. Honda, O. Kitao, H. Nakai, M. Klene, X. Li, J.E. Knox, H.P. Hratchian, J.B. Cross, V. Bakken, C. Adamo, J. Jaramillo, R. Gomperts, R.E. Stratmann, O. Yazyev, A.J. Austin, R. Cammi, C. Pomelli, J.W. Ochterski, P.Y. Ayala, K. Morokuma, G.A. Voth, P. Salvador, J.J. Dannenberg, V.G. Zakrzewski, S. Dapprich, A.D. Daniels, M.C. Strain, O. Farkas, D.K. Malick, A.D. Rabuck, K. Raghavachari, J.B. Foresman, J.V. Ortiz, Q. Cui, A.G. Baboul, S. Clifford, J. Cioslowski, B.B. Stefanov, G. Liu, A. Liashenko, P. Piskorz, I. Komaromi, R.L. Martin, D.J. Fox, T. Keith, M.A. Al-Laham, C.Y. Peng, A. Nanayakkara, M. Challacombe, P.M.W. Gill, B. Johnson, W. Chen, M.W. Wong, C. Gonzalez, J.A. Pople, Gaussian 03, Gaussian Inc., Wallingford, CT, 2004.
[66] P.J. Linstrom, W.G. Mallard (Ed.)(Eds.), NIST Chemistry WebBook, NIST Standard Reference Database Number 69, National institute of Standards and Technology, Gaithersburg MD, 20899 (http://webbook.nist.gov/), June 2005.
[67] E.D. Glendening, A.E. Reed, J.E. Carpenter, F. Weinhold, NBO Version 3.1.
[68] R.H. Petrmichl, K.A. Peterson, R.C. Woods, J. Chem. Phys. 89 (1988) 5454.
[69] W.Y. Fan, Z. Liu, P.B. Davies, J. Mol. Spectrosc. 191 (1998) 98.
[70] M. Ishiguro, T. Okabayashi, M. Tanimoto, J. Mol. Struct. 352/353 (1995) 317.
[71] G. Herzberg, A. Lagerqvist, B.J. McKenzie, Can. J. Phys. 47 (1971) 1889.
[72] N.P.C. Westwood, Chem. Phys. Lett. 25 (1974) 558.
[73] H.R. Ihle, C.H. Wu, M. Miletic, K.F. Zmbov, Adv. Mass. Spectrom. 7 (1978) 670.
[74] V.H. Bock, B. Solouki, G. Maier, Angew. Chem. 97 (1985) 205.
[75] J.C. Creasey, I.R. Lambert, R.P. Tuckett, J. Chem. Soc. Faraday Trans. 87 (1991) 3717.
[76] M. Farber, R.D. Srivastava, High Temp. Sci. 12 (1980) 21.
[77] J.M. Dyke, E.P.F. Lee, A. Morris, L. Nyulaszi, J. Elec. Spectrosc. Rel. Phenom. 66 (1993) 175.
[78] J.M. Dyke, N. Jonathan, A. Morris, A. Ridha, M.J. Winter, Chem. Phys. 81 (1983) 481.
[79] J.H.D. Eland, Photoelectron Spectroscopy: An Introduction to Ultraviolet Photoelectron Spectroscopy in the Gas Phase, Butterworths & Co., Boston, 1984.
[80] P.J. Bassett, D.R. Lloyd, Chem. Phys. Lett. 3 (1969) 22.
[81] P.J. Bassett, D.R. Lloyd, J. Chem. Soc. A (1971) 641.
[82] W.E. Bull, B.P. Pullen, F.A. Grimm, W.E. Moddeman, G.K. Schweitzer, T.A. Carlson, Inorg. Chem. 9 (1970) 2472.
[83] T.P. Fehlner, D.W. Turner, Inorg. Chem. 13 (1974) 754.
[84] R. Basner, M. Gutkin, J. Mahoney, V. Tarnovsky, H. Deutsch, K. Becker, J. Chem. Phys. 123 (2005) 054313.
[85] M. Sana, M. Decrem, G. Leroy, M.T. Nguyen, L.G. Vanquickenborne, J. Chem. Soc. Faraday Trans. 90 (1994) 3505.
[86] D.C. Frost, F.G. Herring, A. Katrib, R.A.N. McLean, N.P.C. Westwood, Can. J. Chem. 49 (1971) 4033.
[87] S. Cradock, E.A.V. Ebsworth, Chem. Commun. (1971) 57.
[88] S. Cradock, R.A. Whiteford, J. Chem. Soc. Faraday Trans. 67 (1971) 3425.
[89] W.B. Perry, W.L. Jolly, J. Elec. Spectrosc. Rel. Phenom. 4 (1974) 219.
[90] S. Cradock, E.A.V. Ebsworth, R.A. Whiteford, J. Chem. Soc. Dalton Trans. 22 (1973) 2401.
[91] T.M. Cheng, F.W. Lampe, Chem. Phys. Lett. 19 (1973) 532.
[92] Y. Ling, R.K. Milbrum, A.C. Hopkinson, D.K. Bohme, J. Am. Soc. Mass Spectrom. 10 (1999) 848.
[93] L.A. Nicolaides, A. Rauk, M.N. Glukhovtsev, L. Radom, J. Phys. Chem. 100 (1996) 17460.
[94] E.P. Hunter, S.G. Lias, J. Phys. Chem. Ref. Data 27 (1998) 413.
[95] K.A. Peterson, T.H.J. Dunning, J. Chem. Phys. 117 (2002) 10548.
[96] S.R. Gunn, L.G. Green, J. Phys. Chem. 65 (1961) 779.
[97] S.R. Gunn, L.G. Green, J. Phys. Chem. 68 (1964) 946.
[98] P. Ho, M.E. Coltrin, J.S. Binkley, C.F. Melius, J. Phys. Chem. 90 (1986) 3399.
[99] A.F. Sax, J. Kalcher, J. Phys. Chem. 95 (1991) 1768.
[100] G. Katzer, M.C. Ernst, A.F. Sax, J. Kalcher, J. Phys. Chem. A 101 (1997) 3942.
[101] M.T. Swihart, S.L. Girshick, J. Phys. Chem. B 103 (1999) 64.
[102] H.-W. Wong, J.C.A. Nieto, M.T. Swihart, L.J. Broadbelt, J. Phys. Chem. A 108 (2004) 874.
[103] M. Farber, R.D. Srivastava, Chem. Phys. Lett. 51 (1977) 307.
[104] M. Farber, R.D. Srivastava, J. Chem. Thermodynam. 11 (1979) 939.
[105] M. Farber, R.D. Srivastava, Chem. Phys. Lett. 60 (1979) 216.
[106] J.M. Jasinski, R. Becerra, R. Walsh, Chem. Rev. 95 (1995) 1203.
[107] A.E. Douglas, B.L. Lutz, Can. J. Phys. 48 (1970) 247.
[108] S.P. Walch, C.E. Dateo, J. Phys. Chem. A 105 (2001) 2015.
[109] K.L. Walker, R.E. Jardine, M.A. Ring, H.E. O'Neal, Int. J. Chem. Kinet. 30 (1998) 69.
[110] C.W.J. Bauschlicher, A. Ricca, J. Phys. Chem. A 103 (1998) 4313.
[111] A. Olsen, F.R. Sale, J. Less-Common Met. 53 (1977) 277.